Title

Nitrogen Deposition Weakens Soil Carbon Control of Nitrogen Dynamics Across the Contiguous United States

Journal

Global Change Biology, 30(12)

ISSN

1354-1013

Authors

Nieland, Matthew A

Lacy, Piper

Allison, Steven D

et al.

Publication Date

2024-12-01

DOI

10.1111/gcb.70016

Title: Nitrogen deposition weakens soil carbon control of nitrogen dynamics across the contiguous United States

Authors: Matthew A. Nieland[1], Piper Lacy[1], Steven D. Allison[2,3], Jennifer M. Bhatnagar[4], Danica A. Doroski[5], Serita D. Frey[6], Kristen Greaney[7], Sarah E. Hobbie[8], Sara E. Kuebbing[9,10], David B. Lewis[11], Marshall D. McDaniel[12], Steven S. Perakis[13], Steve M. Raciti[7], Alanna N. Shaw[14], Christine D. Sprunger[15,16,17], Michael S. Strickland[18,19], Pamela H. Templer[4], Corinne Vietorisz[4], Elisabeth B. Ward[20], Ashley D. Keiser[1]

Affiliations:

[1]Stockbridge School of Agriculture, University of Massachusetts Amherst, Amherst, Massachusetts, USA

[2]Department of Ecology and Evolutionary Biology, University of California, Irvine, Irvine, California, USA

[3]Department of Earth System Science, University of California, Irvine, Irvine, California, USA

[4]Department of Biology, Boston University, Boston, Massachusetts, USA

[5]Connnecticut Department of Energy and Environmental Protection, Hartford, Connecticut, USA

[6]Center for Soil Biogeochemistry and Microbial Ecology, Department of Natural Resources and the Environment, University of New Hampshire, Durham, New Hampshire, USA

[7]Department of Biology, Hofstra University, Hempstead, New York, USA

[8]Department of Ecology, Evolution and Behavior, University of Minnesota, St. Paul, Minnesota, USA

[9]Botany Department, Carnegie Museum of Natural History, Pittsburgh, Pennsylvania, USA

[10]The Forest School at the Yale School of the Environment, Yale University, New Haven, Connecticut, USA

[11]Department of Integrative Biology, University of South Florida, Tampa, Florida, USA

[12]Department of Agronomy, Iowa State University, Ames, Iowa, USA

[13]U.S. Geological Survey, Forest and Rangeland Ecosystem Science Center, Corvallis, Oregon, USA

[14]Montana Department of Environmental Quality, Helena, Montana USA

[15]W.K. Kellogg Biological Station, Michigan State University, Hickory Corners, Michigan, USA

[16]Department of Plant, Soil, and Microbial Sciences, Michigan State University, East Lansing, Michigan, USA

[17]Plant Resilience Institute, Michigan State University, East Lansing, Michigan, USA

[18]Department of Soil and Water Systems, University of Idaho, Moscow, Idaho, USA

[19]Deep Soil Ecotron, University of Idaho, Moscow, Idaho, USA

[20]Department of Environmental Science and Forestry, The Connecticut Agricultural Experiment Station, New Haven, Connecticut, USA

[*]Corresponding Author:
Matthew A. Nieland
mnieland@umass.edu

Key words: air quality, coupled carbon-nitrogen, COVID-19, net nitrogen mineralization, net nitrification, extracellular enzyme activity

Abstract

Anthropogenic nitrogen (N) deposition is unequally distributed across space and time, with inputs to terrestrial ecosystems impacted by industry regulations and variation in human activity. Soil carbon (C) content normally controls the fraction of mineralized N that is nitrified ($f_{\text{nitrified}}$), affecting N bioavailability for plants and microbes. However, it is unknown whether N deposition has modified the relationships between soil C, net N mineralization, and net nitrification. To test whether N deposition alters the relationship between soil C and net N transformations, we collected soils from coniferous and deciduous forests, grasslands, and residential yards in 14 regions across the contiguous U.S. that vary in N deposition rates. We quantified rates of net nitrification and N mineralization, soil chemistry (soil C, N, and pH), and microbial biomass and function (as beta-glucosidase (BG) and *N*-acetylglucosaminidase (NAG) activity) across these regions. Following expectations, soil C was a driver of $f_{\text{nitrified}}$ across regions, whereby increasing soil C resulted in a decline in net nitrification and $f_{\text{nitrified}}$. The $f_{\text{nitrified}}$ value increased with lower microbial enzymatic investment in N acquisition (increasing BG:NAG ratio) and lower active microbial biomass, providing some evidence that heterotrophic microbial N demand controls the ammonium pool for nitrifiers. However, higher total N deposition increased $f_{\text{nitrified}}$, including for high soil C sites predicted to have low $f_{\text{nitrified}}$, which decreased the role of soil C as a predictor of $f_{\text{nitrified}}$. Notably, the drop in contemporary atmospheric N deposition rates during the 2020 COVID-19 pandemic did not weaken the effect of N deposition on relationships between soil C and $f_{\text{nitrified}}$. Our results suggest N deposition can disrupt the relationship between soil C and net N transformations, with this change potentially explained by weaker microbial competition for N. Therefore, past N inputs and soil C should be used together to predict N dynamics across terrestrial ecosystems.

Introduction

The rise in agricultural production and fossil fuel combustion during the 20th century increased nitrogen (N) emissions and, consequently, atmospheric N deposition to terrestrial ecosystems across the globe (Fixen & West, 2002; Gruber & Galloway, 2008). This deposition caused widespread negative environmental impacts, including elevated nitrate (NO_3^-) leaching and nitrous oxide (N_2O) emissions (Schlesinger, 2009; Vitousek et al., 1997). As such, legislative efforts were imposed to curb these atmospheric N inputs. Air quality regulations in the U.S. cut emissions of nitrous oxides (NO_x) by 41% from 1990 to 2010 (Li et al., 2016), reducing inorganic N deposition by 0.11 kg N ha^{-1} yr^{-1} in the eastern U.S. during this period (Ackerman et al., 2019). Although inorganic N deposition rose 8% globally from 1984 to 2016, regions like Europe and Central Indo-Pacific had downward trends in N deposition (Ackerman et al., 2019). The drop in anthropogenic N deposition, combined with elevated atmospheric CO_2 concentrations, can reduce N availability for plants and soil microbes (Garten et al., 2011; Norby et al., 2010; Olff et al., 2022), with emerging evidence suggesting unmanaged ecosystems worldwide are returning to N-limited states (Mason et al., 2022; McLauchlan et al., 2017). The long-term decline in reactive N deposition likely affects ecosystem functions, including decomposition and nitrification. Yet, much remains to be discovered about the variable effects of N deposition across space and time on the microbially-mediated N cycle and its relationship with soil carbon (C).

Aside from bioavailable N derived from atmospheric deposition, terrestrial N availability is controlled by soil microbial communities. Heterotrophic soil microorganisms use extracellular enzymes to break down soil organic matter (SOM) for energy and materials (Burns, 1982; Sinsabaugh, 1994). Microbial enzyme production facilitates N mineralization in soils by

93 converting simple organic N compounds from plants and microbes (including N-fixing bacteria)
94 to ammonium (NH_4^+). Ammonium may then be oxidized by chemolithoautotrophic nitrifiers into
95 NO_3^-, with the potential to be leached into adjacent waterways or lost as the potent greenhouse
96 gas nitrous oxide (N_2O). Both ammonium and nitrate can be immobilized by heterotrophic
97 microbes or taken up by plants to meet N demands (Melillo et al., 1989; Soong et al., 2020).
98 Additionally, larger soil C pools increase heterotrophic N demand to maintain their C:N
99 stoichiometry (Cleveland & Liptzin, 2007; Redfield, 1958; Schimel & Weintraub, 2003), leading
100 to increased N mineralization and immobilization rates but decreased nitrification rates. While
101 site-dependent variables like soil moisture and NH_4^+ do drive nitrification rates, it has been
102 shown at local (Keiser et al., 2016) and continental (Gill et al., 2023) scales from laboratory
103 incubations and field-based assays that soil C content determines whether or not mineralized N
104 (NH_4^+) is nitrified. Specifically, the fraction of mineralized N that is nitrified ($f_{\text{nitrified}}$) is lower
105 under high soil C conditions, likely driven by heterotrophic N immobilization (Elrys et al.,
106 2021), reducing NH_4^+ availability for nitrifiers. As a result, net N mineralization and nitrification
107 rates can become decoupled under high microbially-available C conditions. However, large
108 pulses of external N inputs (e.g., fertilizer application) may exceed heterotrophic N demand,
109 resulting in high nitrification rates and $f_{\text{nitrified}}$ across an array of soil C concentrations as
110 competition for N eases between microbial heterotrophs and nitrifiers (Aber et al., 1998; Yuan et
111 al., 2019). While it is expected that an increase in N availability will increase nitrification rates,
112 the effects of atmospheric N deposition on the role of soil C in mediating $f_{\text{nitrified}}$ has not been
113 resolved.

114 To identify how the activity of soil microorganisms shifts with N availability, we can
115 quantify changes in their functional attributes that characterize their C- and N-cycling potentials,

including extracellular enzyme activity. Field experiments show that N-acquiring enzyme activity declines with concomitant increases in C-acquisition enzyme activity under experimental N-fertilization rates ranging from 30-100 kg N ha^{-1} yr^{-1} (Ajwa et al., 1999; Saiya-Cork et al., 2002; Zeglin et al., 2007). These studies suggest that experimental N fertilization rates—typically greater than realized N deposition rates—lower the enzymatic investment to acquire N by soil microbes, indicative of lower microbial N limitation. In addition, decomposition measures, such as litter mass loss and microbial respiration, decrease with experimentally higher N availability (Craine et al., 2007; Knorr et al., 2005; Treseder, 2008). A decline in decomposition due to decreased microbial N limitation may increase SOM pools as heterotrophic microbes rely less on this organic pool for N (Bowden et al., 2019). Yet, studies report contrasting effects of N-addition on soil C stocks. In forests, chronic N fertilization increases the stock of organic C in the topsoil layer (Frey et al., 2014), whereas soil C stocks do not change in grassland N-addition experiments (Keller et al., 2022). This distinction between forest and grassland soils not only reveals key differences in soil microbial communities between these systems (Carson et al., 2019; Edwards et al., 2011; Frey et al., 2004), but also the importance of understanding what mechanisms govern microbial responses to higher N availability across ecosystems, including edaphic properties known to affect the N cycle, such as soil pH (Kemmitt et al., 2006; Riggs & Hobbie, 2016).

As N deposition decreases in response to environmental regulations, ecosystem recovery may lag behind this decline (Gilliam et al., 2019; Stevens, 2016) given that ecosystems retain exogenous N in plant and soil pools (Lovett & Goodale, 2011). From the few field experiments where high rates of N fertilization has ceased and observations have continued, N mineralization rates have been shown to remain elevated for over five years compared to never-fertilized

controls (Clark et al., 2009; O'Sullivan et al., 2011), but pre-fertilization nitrification rates can recover in one year (Nieland et al., 2021). Yet, these experiments coincide with the slow, multidecadal decline in N deposition in many regions and concurrent rise in atmospheric CO_2 concentrations, with studies without experimental N fertilization reporting decreases in plant tissue N concentrations and natural abundance $\delta^{15}N$ values, ecosystem N-cycling rates, and aquatic N exports from watersheds (Groffman et al., 2018; Penuelas et al., 2020; Sabo et al., 2020). The observational N fertilization studies instead suggest that legacies of anthropogenic N deposition may not be realized in natural systems because contemporary atmospheric chemistry, specifically CO_2 fertilization, appears to have a stronger role in ecosystem N-cycling than previous N deposition. With limited experimental data matching low and variable rates of N deposition, it remains uncertain as to how soil microbial communities respond functionally to decreased anthropogenic N deposition across diverse ecosystems (Lamarque et al., 2013).

The COVID-19 pandemic prompted a sudden drop in human activity around the globe as 2020 lockdowns restricted work and outdoor activities in an attempt to slow the spread of SARS-CoV-2 (Alfano & Ercolano, 2020), the virus that causes COVID-19. Consequently, 2020 vehicular traffic and industry activity decreased (Liu & Stern, 2021) with increases in select air quality metrics (i.e., $PM_{2.5}$, PM_{10}, NO_2; Yang et al., 2022) and avian and beach flora and fauna abundances across urban ecosystems (Schrimpf et al., 2021; Soto et al., 2021). However, the effects of the COVID-19 pandemic on terrestrial biogeochemistry are not known, despite reported declines in atmospheric N deposition (Berman & Ebisu, 2020; Le Quéré et al., 2020). This 'anthropause' (Rutz et al., 2020) presents the opportunity to investigate whether a short-term decrease in N deposition during 2020 alters the relationships between soil C, net N mineralization, and net nitrification and the strength of soil C as a driver of $f_{\text{nitrified}}$.

Taking advantage of both the decline in rates of atmospheric N deposition during the COVID-19 pandemic and the range in background atmospheric N deposition across the contiguous U.S., we examined under laboratory conditions if N deposition alleviates soil C-controlled competition for N between microbial heterotrophs and nitrifiers. We sampled 14 regions (with multiple sites per region) experiencing variable N deposition rates (annual means: 3.2-11.7 kg N ha^{-1} yr^{-1}), and measured soil net nitrification and N mineralization rates, extracellular enzyme activities (EEAs), active microbial biomass with substrate induced respiration (SIR), and soil chemistry (soil C, N, and pH). We hypothesized (H1) that high C soils with high background rates of atmospheric N deposition exhibit higher net nitrification rates and $f_{\text{nitrified}}$ than high C soils with low background N deposition because NH_4^+ supplied through deposition would alleviate NH_4^+-limitation of nitrifiers induced by immobilization (Fig. 1a, b). Initiating the study during the COVID-19 pandemic, we leveraged this natural experiment to discern if a short-term dip in contemporary N deposition decreased $f_{\text{nitrified}}$. We hypothesized (H2) that a temporary decrease in N deposition strengthens the role of soil C in regulating net N transformation rates and $f_{\text{nitrified}}$, resulting in a decrease in net N transformation rates and $f_{\text{nitrified}}$, because microbial immobilization would drive NH_4^+-limitation for nitrifiers at sites where background N deposition rates are typically at intermediate or high levels (Fig. 1c).

Methods

Study sites and sample collection

We sampled soils from 14 regions across the U.S. that varied in rates of atmospheric N deposition and climate (Table S1). Each region included individual sites that captured a range of vegetation and land uses, including forest, grassland, and residential yard, for a total of 39 sites.

185 At a minimum, each region had one natural ecosystem reflecting the area's dominant ecosystem
186 type and one residential yard. We included yards because they offer a relatively similar
187 comparison, in terms of vegetation, across the 14 regions and climates, and most yards shared
188 similar management across regions (Table S1). We classified non-yard sites into coniferous
189 forest, deciduous forest, grassland, scrub, and oak-palmetto forest ecosystems based on
190 vegetation and climate. 30-year mean annual precipitation (MAP) and temperature (MAT) were
191 estimated for each site using the closest weather station in the National Weather Service
192 Cooperative Network (NWS COOP). Monthly precipitation (PPT) and potential
193 evapotranspiration (PET) during 2013-2021 were calculated to identify climate (i.e., mesic or
194 xeric) using daily precipitation, daily maximum and minimum temperatures, and latitude (for
195 solar radiation; Allen et al., 1999). A PPT:PET ratio of less than one was defined as a xeric
196 climate (Knapp et al., 2008).
197 Samples were collected by taking the top 10 cm of mineral soil with a trowel to fill
198 approximately a quart-size (0.95 L) sterile bag four times at each site in 2020. These collection
199 times were selected to correspond with changes in national activity due to COVID-19 restrictions
200 in 2020 (with increasing human activity across time): April (stay-at-home), May (partial
201 reopening), June, and August. Each sample was split in half with one sub-sample immediately
202 frozen and the other air-dried. Once COVID-19 restrictions lifted, dried and frozen samples were
203 shipped to the University of Massachusetts Amherst where frozen samples remained at -20 ºC
204 until processed. For this study, we analyzed soils from the first and fourth collections to capture
205 the timepoints with the widest range in COVID restrictions and potential for contrasting N
206 deposition rates. Because some sites included replicated plots, samples from plot replicates were
207 processed separately and then averaged within a site for data analysis. Samples were collected at

a subset of the sites a year after the initial collections in 2021 to determine if changes in local deposition levels affected soil microbial functions. While the seven sites resampled were collected from the Northeastern U.S., because of their proximity to the University of Massachusetts Amherst, we only used these sites to compare soil functional parameters between a year with reduced human activity (2020) and a year with closer to normal activity (2021). For these samples, we kept plot replicates separate for data analysis.

Atmospheric nitrogen deposition estimates

Annual total (wet + dry) N deposition and wet NH_4^+ deposition were estimated for each site using model outputs detailed in Schwede and Lear (2014). Grids from the National Atmospheric Deposition Program's (NADP) National Trends Network (NTN) (version 2023.01; https://nadp.slh.wisc.edu/committees/tdep/) were accessed on November 14, 2023, and uploaded to RStudio V2023.12.1+402 (Posit team, 2024) using R package *raster* (Hijmans 2023). We collected deposition data from online databases covering 2013-2021 (pre-study years plus study period). While an expected decrease in deposition induced by the COVID-19 pandemic inspired the current study, preliminary data analysis indicated that annual N deposition rates declined in 2018 and through 2020, before rebounding in 2021. Because we wanted to investigate both background and contemporary N deposition effects motivated by the COVID-19 restrictions, we defined background N deposition as 2013-2017 before N deposition began to decline. Using the 2013-2017 values, we averaged annual total N deposition estimates for each of the 39 sites to define 'low' (2013-2017 mean site total N deposition range: 3.18-6.93 kg N ha^{-1} yr^{-1}), 'intermediate' (7.53-8.45 kg N ha^{-1} yr^{-1}), and 'high' (8.56-11.67 kg N ha^{-1} yr^{-1}) background rates of N deposition from the 33rd and 66th percentiles of the mean rates of N deposition. We binned

231 background N deposition into ranks because preliminary analyses of 2013-2017 mean site N
232 deposition rates showed three distinct groups, which approximately aligned with the 33rd and 66th
233 percentiles. Each N deposition rank included 13 sites. Average annual NH_4^+ deposition was also
234 calculated for each site.
235 The decline in human activity from the COVID-19 pandemic presented unique
236 challenges to quantifying real-time wet N deposition declines because many NTN stations were
237 closed during this time. Therefore, we used the automated United States Environmental
238 Protection Agency (EPA) Clean Air Status and Trends Network (CASTNET)
239 (https://epa.gov/castnet/) to gather particulate (dry) N deposition data since CASTNET stations
240 were not disrupted during the lockdown period of spring 2020. We extracted weekly CASTNET
241 dry N concentration data from 2013-2021 on February 14, 2024, from six stations. These stations
242 were selected because of their proximity to sampling locations and variation in total background
243 N deposition rates (Fig. S1). With the CASTNET data, we first calculated dry N deposition flux
244 using deposition velocities reported in Holland et al. (2005) and then added the fluxes to report
245 annual cumulative dry N deposition. As with total N deposition, 2013-2017 served as
246 background years to calculate the 95% confidence interval for dry N deposition. Dry N
247 deposition in 2018-2021 that fell outside the confidence intervals was considered significantly
248 different from background N deposition at $P \leq 0.05$. The fraction of annual total N deposition
249 deposited as dry N, based on the 2013-2017 NTN and CASTNET data, ranged from (mean ±
250 standard deviation) 10.4 ± 2.2% in northern Montana to 61.7 ± 4.9% in southern California
251 (overall mean: 22.4%). Thus, we are somewhat limited in our inference about the potential
252 change in total N deposition during the early part of the COVID-19 pandemic due to missing wet
253 N deposition data in 2020. However, dry N deposition serves as a good indicator for vehicular

activity since dry N deposition is higher in urban sites (Bettez & Groffman, 2013) and deposition rates decline exponentially away from roads (Redling et al., 2013), with some notable exceptions (Rocci et al., 2023).

Soil chemistry

Air-dried soils were sieved to 2 mm and then pulverized using a CertiPrep 8000-D Mixer mill (Spex, Mutuchen, NJ, USA), and total C and N from two milled analytical replicates were quantified using a Carlo Erba NA1500 CHN analyzer (Thermo Fisher Scientific, Waltham, MA, USA). Soils with ≤ 5% C (by mass) were defined as low C soils (Gill et al., 2023). Soil C and N were transformed to molar quantities to calculate soil C:N ratios. A portion of the frozen soil was thawed and sieved to 2 mm, and the pH was measured in a 1:2 volumetric ratio of soil and deionized water (Allen, 1974). Soil moisture was measured as gravimetric water content (GWC), quantified by drying soils for 24 h at 105ºC (Bradford et al., 2008).

Soil microbial carbon and nitrogen cycling

Functional assessments of microbial communities were measured from thawed soils previously frozen at -20°C. Net N mineralization and nitrification rates were measured using a 28-d lab incubation (Robertson & Groffman, 2015). Immediately after sieving to 2 mm, 10 g dry-equivalent soil were added to 50 mL of 2 M KCl and shaken vigorously by hand (day 0) (Keiser et al., 2016; Robertson et al., 1999). Another 10 g dry-equivalent soil were incubated at 20 ºC in the dark for 28 days and checked weekly to maintain soil moisture at gravimetric moisture from field collection. At day 28, the soil was extracted in 50 mL of 2 M KCl and shaken. Inorganic N concentrations (NH_4^+-N and NO_3^--N) were quantified

277 spectrophotometrically with a BioTek Synergy HTX Multimode Reader (Agilent, Santa Clara,
278 CA, USA) using a modified salicylate assay and vanadium (III) assay, respectively (Hood-
279 Nowotny et al., 2010). Net N mineralization rates were calculated as the difference in total
280 inorganic N after 28 days, while nitrification rates were calculated as the difference in NO_3^--N.
281 The nitrified fraction of mineralized N ($f_{nitrified}$) was calculated by dividing net nitrification rate
282 by net N mineralization rate.
283 We measured substrate induced respiration (SIR) as an estimate of active soil microbial
284 biomass. SIR was measured after shaking 5 g dry-equivalent soil with autolyzed yeast solution
285 for 1 h at 100 rpm inside capped, 50 mL tubes with 2 replicates per sample (Anderson &
286 Domsch, 1978; Bradford, Fierer, et al., 2008). After a 4 h incubation, CO_2-C in the headspace
287 was quantified using a LI-7000 CO_2/H_2O analyzer (LICOR, Lincoln, NE, USA).
288 Soil EEAs were measured using short-term, room-temperature assays with fluorometric
289 methylumbelliferone (MUB) substrates in a modified universal buffer at a given soil's pH
290 (German et al., 2011; Saiya-Cork et al., 2002). Beta-glucosidase (BG; EC 3.2.1.21) and *N*-
291 acetylglucosaminidase (NAG; EC 3.2.1.14) activities were measured in 96-well plates with 8
292 replicates for each enzyme per sample and included MUB curves, substrate controls, and soil
293 homogenate controls. Prior to these assays, K_m tests for each site were performed to determine
294 the times and substrate concentrations to achieve the maximum reaction rate (V_{max}) (Keiser et al.,
295 2019). Fluorescence was measured at 360/450 nm (excitation/emission) with a BioTek Synergy
296 HTX Multimode Reader. To evaluate microbial enzymatic investment for labile C and N, we
297 calculated the ratio of BG and NAG activities, both natural-log transformed, with lower ratios
298 indicative of higher N relative to C demand (Nieland et al., 2024; Sinsabaugh & Follstad Shah,
299 2012).

300

301 *Statistical analysis*

302 All statistical analyses were done in R V4.3.3 (R Core Team, 2024) using *tidyverse* to
303 handle and visualize data (Wickham et al., 2019). We used linear mixed effects (LME) models
304 and linear models for all analyses. To test for differences in background N deposition, we first
305 used linear models to determine if mean annual background total N deposition and wet NH_4^+
306 deposition from 2013-2017 were different among the low, intermediate, and high deposition
307 ranks. We then assessed whether total N and wet NH_4^+ deposition decreased from 2013-2017 by
308 using LME models that included N deposition rank (low, intermediate, and high N deposition)
309 and years as interacting fixed effects with sites being random effects to account for repeating
310 measurements using packages *lme4* and *lmerTest* (Bates et al., 2015; Kuznetsova et al., 2017).
311 We used stepwise modeling to identify linear models that describe net nitrification rates
312 and test H1. Following the Keiser et al. (2016) and Gill et al. (2023) approach, we used model
313 selection among known drivers of nitrification to isolate the best model that describes
314 nitrification, first excluding and then including background N deposition. The first model
315 selection exercise tested for the best model using predictors identified by Keiser et al. (2016) and
316 tested at a continental scale by Gill et al. (2023): net N mineralization rates, soil C, and GWC as
317 interacting explanatory variables. Using Akaike information criterion (AIC) from the R package
318 *MASS* to remove variables (Venables & Ripley, 2002), the best fit model included net N
319 mineralization rate, soil C, soil moisture, and the interaction of N mineralization rate and soil
320 moisture as predictive variables for net nitrification rates (Adjusted $R^2 = 0.313$, $P < 0.001$, AIC =
321 193.6). The second model selection exercise included background (2013-2017) total N
322 deposition as a variable, along with net N mineralization rates, soil C, and GWC (allowing them

to interact), to describe net nitrification rates. Background total N deposition, rather than wet NH_4^+, was used because it accounts for other deposited N species that can influence plant-microbe and microbe-microbe competition for N. According to AIC and analysis of variance (ANOVA), the model from the second exercise was a better fit than the model from the first exercise (AIC = 188.0, $P = 0.013$); thus, we report results from the second model.

Additional models were implemented to test H1. Because other soil characteristics can influence nitrification (Keiser et al., 2016), we designed a separate linear model using the stepwise approach to test the effects of net N mineralization, soil moisture, soil pH, soil C, soil C:N, and their interactions on net nitrification rates, which were visualized using the *interactions* R package (Long, 2019). Soil N was excluded due to its collinearity with soil C. Moreover, we used linear models to test if $f_{\text{nitrified}}$ was different between soils with low C and high C and among ecosystem types, including their interaction. We further tested H1 by assessing whether net nitrification and N mineralization rates and $f_{\text{nitrified}}$ were related to soil microbial functions. To do this, we used linear models of net nitrification, net N mineralization, and $f_{\text{nitrified}}$ that separately tested active microbial biomass, log(NAG), and microbial enzymatic C:N investment as fixed effects interacting with N deposition rank.

To further test H1, we built a structural equation model (SEM) to determine how N deposition class (low, intermediate, and high) changed the effects of soil chemistry, particularly soil C, and microbial functions on $f_{\text{nitrified}}$. We first designed model paths *a priori* from existing literature (Fig. S2, Table S2) and added linear models into an SEM using the *piecewiseSEM* package (Lefcheck, 2016). We then checked the fit of the SEM using χ^2 and Fisher's C statistics which showed that the data fit poorly to the SEM ($\chi^2 = 25.37$, df = 6, $P < 0.001$; Fisher's C = 28.74, df = 12, $P = 0.004$). A d-separation test (Shipley, 2013) indicated that adding a path

between microbial enzymatic C:N investment and soil pH to the SEM would improve fit. In addition, a linear model predicting $f_{\text{nitrified}}$ from soil moisture was unnecessary based on its *P*-value ($P = 0.555$); we subsequently removed this linear model from the SEM. After making these changes, the overall fit of the SEM improved ($\chi^2 = 3.61$, df = 3, $P = 0.307$; Fisher's C = 5.12, df = 6, $P = 0.529$). We tested if N deposition class changed the magnitude of effects by performing a multigroup analysis using the multigroup function in *piecewiseSEM*. Standardized coefficients and *P*-values were gathered to compare outputs of each N deposition class, and we calculated the direct, indirect, and total effect of soil C on $f_{\text{nitrified}}$ among each N deposition class.

For H2, we used LME models to assess whether there were differences in net N nitrification and N mineralization rates between 2020 and 2021 for the resampled sites with individual plots as a random effect. These LME models included site, collection, and year as interacting fixed effects. We further tested H2 by using an LME model to test for differences in $f_{\text{nitrified}}$ between year and soil C as interacting fixed terms, with plot as a random effect.

To test if soil characteristics varied across sites, we used stepwise modeling to select the best fitting linear model for the response variables soil pH, soil %C, soil %N, and soil C:N. Model predictors included climate (xeric or mesic), ecosystem (coniferous forest, deciduous forest, grassland, or residential yard), and deposition rank. We also modeled soil moisture as a function of these factors, excluding N deposition rank. Background N deposition was modeled as a categorical rather than continuous variable for ease of interpretation, and scrub and oak-palmetto forest ecosystems were excluded due to low replication. Two-way interactions among all predictor variables were included in the models. To meet model assumptions, some response variables were natural-log transformed or expressed using Yeo-Johnson transformation (Table S3 and S4). ANOVA approximations were used to acquire *F*- and *P*-values for models, and

significant effects or interactions were tested using Tukey's post-hoc analysis in package *emmeans* (Lenth, 2023). Significance was set at $\alpha \leq 0.05$.

Results

Nitrogen deposition

Background total (wet + dry) N deposition rates (2013-2017) varied strongly across the contiguous U.S., ranging over an order of magnitude among our 39 sites in 14 regions (Fig. 2a). Most of the high background N deposition sites were in the Midwest (n = 6; 9.8 ± 0.4 kg N ha^{-1} yr^{-1}), and all the sites in Northern Rockies and California (n = 10; 4.7 ± 1.4 kg N ha^{-1} yr^{-1}) had low background N deposition. Background total N deposition rates increased significantly from the low to intermediate to high classes (all $P < 0.001$). Regardless of deposition class, however, total N deposition rates declined annually 0.14 kg N ha^{-1} yr^{-1} from 2013-2017 ($F_{1,153} = 10.9$, $P = 0.001$; Fig. 2b) consistent with other studies (Ackerman et al., 2019; Benish et al., 2022). High N deposition sites had higher mean annual wet NH_4^+ deposition (2.9 ± 1.1 kg NH_4^+-N ha^{-1} yr^{-1}) than low (1.1 ± 0.4 kg NH_4^+-N ha^{-1} yr^{-1}) and intermediate (1.7± 0.5 kg NH_4^+-N ha^{-1} yr^{-1}) sites ($P < 0.001$), but unlike total N deposition annual wet NH_4^+ deposition rates did not decline from 2013-2017. While cumulative dry N deposition decreased significantly in 2019 from the 2013-2017 mean for three of the six CASTNET stations surveyed, it fell to its the lowest values in 2020 for five stations (Fig. S3). Cumulative dry N deposition returned to 2013-2017 ranges in 2021 (Fig. S3).

Net nitrification and N mineralization rates

Low C soils (< 5% C by mass; Gill et al., 2023) had net nitrification rates that predominantly aligned 1:1 with net N mineralization rates, as indicated by an of $f_{\text{nitrified}} = 1$ (Fig. 3a). Indeed, $f_{\text{nitrified}}$ was two-fold greater in low C soils (0.945) than in high C soils (0.417; $F_{1,60} = 15.87$, $P < 0.001$; Fig. 3c) and was not different among coniferous and deciduous forests and grasslands ($P > 0.05$). Net nitrification rates were very low or undetectable in many of the high C soils, among which net N mineralization rates varied widely, indicating that the net N transformations were highly or entirely decoupled from one another in these soils. Yet, net nitrification and N mineralization rates did not always decouple at high soil C sites, with $f_{\text{nitrified}}$ varying between 0 and 1 (Fig. 3a). The best fit model from the model selection exercises predicting net nitrification rates included background mean N deposition as a covariate ($t = -3.02$, $P = 0.004$; Fig. 3b), along with net N mineralization ($t = 1.09$, $P < 0.001$), soil C ($t = -2.31$, $P = 0.024$), and soil moisture ($t = -1.87$, $P = 0.065$; Adjusted $R^2 = 0.379$). Net nitrification rates were negatively related to soil C as expected (Table 1). Under low soil moisture content, soils with higher net N mineralization rates resulted in higher net nitrification rates ($t = -3.32$, $P = 0.001$). In contrast, net nitrification rates increased with soil moisture at sites with higher mean background N deposition rates but decreased under lower background N deposition ($t = 2.93$, $P = 0.005$).

The model testing the effects of soil characteristics and net N mineralization explained 72% of the variation in net nitrification rates. In this model (Table 2), net N mineralization rates interacted positively with soil pH ($t = 2.86$, $P = 0.006$) and soil C ($t = 2.56$, $P = 0.013$) but negatively with soil C:N ($t = -3.32$, $P = 0.002$) and moisture ($t = -2.10$, $P = 0.04$). Net nitrification rates increased more with higher net N mineralization rates under drier, lower soil

moisture (Fig. S4). However, at any given net N mineralization rate, soils with lower C:N ratios (i.e., more N relative to C) or higher pH had higher net nitrification rates (Fig. S4).

Soil chemistry

Background N deposition classification was identified as a significant predictor for soil pH, total C and N, and soil C:N (Table 3), soil characteristics that also predicted net nitrification rates (Table 2). Except in the case of the soil C:N ratio, N deposition classification also interacted significantly with ecosystem type to explain soil chemistry variation (Table 3). Soil C and N concentrations decreased across increasing N deposition classes for coniferous forests and grasslands by an average 59% and 60%, respectively (Fig. S5; all $P < 0.05$) but did not change for deciduous forests or yards. Collectively, soil C:N ratio declined from intermediate to high N deposition ($P = 0.013$) by 2.2 units, with coniferous and deciduous forests having higher soil C:N ratios than grasslands and yards (Fig. S5; all $P < 0.001$). While coniferous forest soil pH decreased from 6.0 ± 0.4 in low N deposition sites to 4.7 ± 0.9 in intermediate N deposition sites (Fig. S5; $P = 0.006$), yard soil pH instead increased from 6.1 ± 1.1 in low N deposition sites to 7.1 ± 0.5 in high N deposition sites (Fig. S5; $P \leq 0.013$). In contrast to other soil properties, soil moisture was best explained by ecosystem type and time, reflecting that soils were wetter at the first collection than the fourth collection ($F_{1, 64} = 47.02$, $P < 0.001$) and that deciduous forests had the highest soil moisture content at the first collection (all $P < 0.05$). Climate only emerged as a predictor for the soil pH, albeit insignificantly (Table 3).

Soil microbial functions

Microbial enzymatic investment for C relative to N acquisition through the ratio of the C-acquiring enzyme BG with the N-acquiring enzyme NAG (BG:NAG ratio) can be used as a microbial N demand index (Nieland et al., 2024; Sinsabaugh & Follstad Shah, 2012). Our results show that when $f_{\text{nitrified}}$ was low, generally in high C soils, the ratio of BG:NAG was also low, indicating relatively high microbial N demand ($F_{1,68} = 23.42$, $P < 0.001$; Fig. 4a). The relationship between the BG:NAG ratio and net nitrification rates was also positive ($F_{1,68} = 12.10$, $P < 0.001$; Fig. 5a); in contrast, net N mineralization rates decreased under higher BG:NAG ratios (i.e., lower net N mineralization rates with lower relative microbial N demand) ($F_{1,71} = 5.04$, $P = 0.028$; Fig. 5b). Significant interactive effects of background N deposition and NAG activity on net nitrification ($F_{2,71} = 3.21$, $P = 0.046$) and N mineralization rates ($F_{2,71} = 4.12$, $P = 0.02$) signal how background N deposition changed microbially mediated N-cycling. Post-hoc tests show that net nitrification and N mineralization rates increased with NAG activity at low N deposition but decreased at intermediate ($P = 0.045$) and high N deposition ($P = 0.031$), respectively (Fig. S6).

Active microbial biomass associated negatively with $f_{\text{nitrified}}$ ($F_{1,71} = 4.71$, $P = 0.033$), such that a larger active microbial biomass pool led to a smaller fraction of mineralized N that was nitrified (Fig. 4b). However, active microbial biomass interacted significantly with N deposition for net N mineralization ($F_{2,71} = 5.09$, $P = 0.009$), in that the relationship between active microbial biomass and net N mineralization rates switched from positive to negative as background N deposition increased (Fig. 4c; $P = 0.012$).

Structural equation model analysis

457 The SEM revealed that the strength of the relationships between soil C, soil N, microbial
458 biomass, microbial enzymatic C:N, and soil pH with $f_{\text{nitrified}}$ diminished as N deposition
459 increased (Fig. 6). Moving from low to high N deposition classification, the effect sizes of soil
460 chemistry and microbial functions on $f_{\text{nitrified}}$ and its predictors generally declined and became
461 insignificant (Fig 6a-c). The direct effect of soil C on $f_{\text{nitrified}}$ was significantly negative while
462 N concentration effects were significantly positive at low N deposition (Fig. 6a). However, soil
463 C was not significantly associated with $f_{\text{nitrified}}$ at intermediate and high N deposition, with only
464 soil pH being positively related to $f_{\text{nitrified}}$ at intermediate N deposition. Collectively, the total
465 (direct + indirect) effect of soil C on $f_{\text{nitrified}}$ decreased with increasing N deposition
466 classification (Fig. 6d).
467
468 *Interannual variability in net N transformations*
469 Despite a decline in external N inputs in the year 2020 and an increase back to pre-2020
470 rates (2013-2017) in 2021 (Fig. S3), there were no major differences in net N transformation
471 rates between 2020 and 2021 (Fig. 7). Only one of the seven sites (Mixed Forest - N CT) had
472 higher net N mineralization rates in 2021 compared to 2020 (Fig. 7a). A significant three-way
473 interaction between site, time, and year for net nitrification rates ($F_{15,88} = 1.85$, $P = 0.040$)
474 indicated that rates were sometimes higher in 2021 than in 2020 for two sites, with no
475 differences in rates between 2020 and 2021 for the other five sites (Fig. 7b). Four sites had little
476 to no net nitrification in 2020 and 2021, resulting in $f_{\text{nitrified}}$ values close to zero. In contrast, one
477 site (Oak-Hickory - S CT) had a 2020-2021 mean $f_{\text{nitrified}}$ of 0.173 while two sites (Suburban -
478 PA and Urban – PA) had $f_{\text{nitrified}}$ values greater than 1. $f_{\text{nitrified}}$ was greater in 2021 (0.06 ± 0.11)
479 than 2020 (0.02 ± 0.04; $F_{1,84} = 9.76$, $P = 0.002$) but only after excluding the two PA sites from

480 the analysis. When including the PA region, however, $f_{\text{nitrified}}$ decreased in 2021 (0.46 ± 0.74)
481 compared to 2020 (0.77 ± 1.48) because of their greater overall rates compared to the remaining
482 sites ($F_{1,115} = 4.36$, $P = 0.039$). Soil C was an insignificant parameter in explaining net N
483 transformations and $f_{\text{nitrified}}$.
484
485 **Discussion**
486 *Fraction of mineralized N that is nitrified potentially tied to microbial competition*
487 Across an anthropogenic N deposition gradient within the contiguous U.S., we tested
488 whether N deposition weakened soil C control over the coupling between net nitrification and N
489 mineralization rates when plants are excluded. We found that soil C was negatively related to net
490 nitrification rates and resulted in $f_{\text{nitrified}}$ either close to 0 (decoupled N transformations) or 1
491 (coupled N transformations), supporting the hypothesis that soil C controls competition for N
492 between heterotrophic microbes and nitrifiers (Dijkstra et al., 2008). A recent study leveraging
493 Long-Term Ecological Research data across various biomes and climates in North America also
494 documented that soil C influenced the degree of coupling of net N transformations across
495 ecosystems (Gill et al., 2023). Labile C availability primarily regulates how much N is released
496 by microbial heterotrophs (Keiser et al., 2016). Although we did not quantify labile C
497 availability, this pool correlates positively to the measured total soil C (McLauchlan & Hobbie,
498 2004). Moreover, higher soil C:N ratios resulted in much lower net nitrification rates measured
499 using laboratory incubations even under relatively high net N mineralization rates. This finding
500 of low net nitrification rates under high soil C:N environments could be more pronounced in the
501 presence of roots because plants also compete with nitrifiers for NH_4^+, further restricting
502 nitrification. Thus, our analysis across multiple terrestrial ecosystems that vary in soil

503 characteristics and climates offers evidence that soil C availability drives coupled-decoupled net
504 N transformations whereby $f_{\text{nitrified}}$ associates negatively with increasing soil C.

505 Although we did not explicitly measure competition for NH_4^+ in this study using gross
506 rates, our functional assays suggested that competition for N between microbial heterotrophs
507 and nitrifiers appeared to shape soil N dynamics. Soil microorganisms synthesize fewer
508 extracellular enzymes that target SOM for labile N (i.e., NAG) under higher available N
509 conditions as a mechanism to conserve intracellular resources (Allison & Vitousek, 2005;
510 Chróst, 1991; Nieland et al., 2024; Sinsabaugh et al., 2008; Sinsabaugh & Follstad Shah, 2012).
511 Microbial enzymatic investment for C- relative to N-acquisition, the BG:NAG ratio, serves as an
512 indicator of microbial N limitation because it reflects the balance between bioavailable N, largely
513 controlled by plant N uptake and heterotrophic N requirements (Fierer et al., 2021; Sinsabaugh et
514 al., 2009), despite NAG being a C- and N-acquisition enzyme. Lower microbial heterotrophic N
515 demand has been associated with higher net nitrification and mineralization rates (Jia et al.,
516 2020; Jian et al., 2016; Ouyang et al., 2018; Vega Anguiano et al., 2024), and we found some
517 evidence that $f_{\text{nitrified}}$ increased also as microbial N demand decreased (Fig. 4a). However, the
518 SEM indicated that microbial N demand was weakly associated with $f_{\text{nitrified}}$ when other
519 pathways in explaining $f_{\text{nitrified}}$ were also included. This contrast between the SEM and the linear
520 model highlights that other relationships tied to $f_{\text{nitrified}}$ besides microbial N demand measured
521 using extracellular enzymes are necessary to explain how microbial competition for N affects
522 $f_{\text{nitrified}}$.

523 The negative relationship between active microbial biomass and $f_{\text{nitrified}}$ further supports
524 the idea that competition between microbial heterotrophs and nitrifiers may drive the relationship
525 between soil C and net N transformations. Soil microbial heterotrophs compete with nitrifiers for

526 NH_4^+ (Verhagen et al., 1995), with gross immobilization rates exceeding gross nitrification rates
527 in some cases (Hart et al., 1994). A recent synthesis found that soil microbial biomass C,
528 quantified through chloroform fumigation extraction, is a driver of gross N immobilization rates
529 (Li et al., 2021). Hence, greater soil microbial biomass, particularly the active pool measured
530 through SIR, should increase N immobilization and limit nitrification (Li et al., 2020; Schimel &
531 Bennett, 2004). Ectomycorrhizal (EcM) fungi may also play a key role in $f_{\text{nitrified}}$ in soils as these
532 organisms are known to compete with nitrifiers for NH_4^+ (Tatsumi et al., 2020) and associate
533 with trees at some of our sites (Table S1; Phillips et al., 2013). Given that net N mineralization
534 and nitrification rates were measured in the lab, bioavailable N may be greater than would be
535 expected in the presence of roots and their mycorrhizal symbionts . Altogether, our functional
536 assessments of soil microbial communities provide further evidence that the mechanism for net
537 nitrification and N mineralization coupling is explained by microbial competition for NH_4^+.
538
539 *Nitrogen deposition modifies net N transformation dynamics*
540 Background rates of N deposition partially explained net nitrification rates and $f_{\text{nitrified}}$,
541 with $f_{\text{nitrified}}$ increasing under high background N deposition in high soil C, supporting H1 that N
542 deposition alleviates NH_4^+-limitation of nitrifiers (Fig. 1). Previous research found that soil C
543 was the primary driver determining the degree of coupling of net N mineralization and
544 nitrification in terrestrial landscapes (Gill et al., 2023; Keiser et al., 2016). Our analysis suggests
545 that background N deposition explained $f_{\text{nitrified}}$ in addition to soil C. Many of the high soil C
546 sites that deviated from their predicted decoupled net nitrification-N mineralization relationship
547 (i.e., $f_{\text{nitrified}} = 0$) had intermediate or high background N deposition. Moreover, the total effect of
548 soil C on $f_{\text{nitrified}}$ diminished as background N deposition increased. These findings could explain

549 why some high soil C ecosystems reported in Gill et al. (2023) had coupled net N
550 transformations, particularly for the Midwest and Atlantic coast sites where dry deposition of
551 ammonia (NH_3) is high because of agriculture (Liu et al., 2022). Further, these Midwest and
552 Atlantic coast soils were relatively enriched with N based on soil C:N ratios (Fig. S3); thus, net
553 nitrification rates and $f_{\text{nitrified}}$ should increase with more available N (Elrys et al., 2021). Because
554 wet and dry deposition has been NH_4^+-dominated in the U.S. in recent years (Li et al., 2016), N
555 deposition should continue to alleviate NH_4^+-limitation for nitrifiers, with oxidized forms of
556 deposited N supplying N to plants and microbial heterotrophs, weakening competition with
557 nitrifiers.

558 Site-specific characteristics may partially explain net nitrification rates. For example, our
559 analysis showed that under drier soil conditions, high net N mineralization rates resulted in high
560 net nitrification rates. Conversely, soils with high moisture content and high background mean N
561 deposition supported high net nitrification rates even when net N mineralization rates were low.
562 The source of available NH_4^+ for nitrifiers may therefore switch from N mineralization to
563 deposition, and vice versa, under changing soil moisture conditions that could reflect site-
564 specific edaphic characteristics, such as soil texture. However, our inferences on soil moisture
565 and nitrification rates are limited since soil moisture was excluded from the SEM and given that
566 laboratory incubations were run under field moisture conditions rather than at 65% water holding
567 capacity (Linn & Doran, 1984). Another soil characteristic, soil pH, also interacted with net N
568 mineralization rates to explain net nitrification rates. Nitrification activity is generally more
569 favored in neutral soils since NH_3 availability, the substrate for ammonia oxidizers, declines at
570 lower pH conditions due to NH_4^+ ionization (Frijlink et al., 1992). While site-specific soil
571 characteristics influence soil microbial activity (Zeglin et. al, 2007) and N access (Keiser et al.,

572 2016) and can explain some variation in nitrification rates across regions, our analysis reveals the
573 dual control of soil C and background N deposition as potential large-scale drivers of $f_{\text{nitrified}}$.
574 The functional assessments of enzyme activity and active microbial biomass that indicate
575 probable soil microbial competition for N when considered together changed in response to
576 increasing background N deposition. At low N deposition, active microbial biomass and net N
577 transformations rates were positively related as expected (García-Ruiz et al., 2008; Hobbie,
578 2015), with the SEM confirming the negative association with active microbial biomass and
579 $f_{\text{nitrified}}$. However, at intermediate and high N deposition, active microbial biomass and NAG
580 activity correlations with net N transformations unexpectedly turned negative, as well as active
581 microbial biomass insignificantly relating to $f_{\text{nitrified}}$ in the SEM. A recent meta-analysis reports
582 NAG activity is suppressed at N application rates at or exceeding 83 kg N ha^{-1} y^{-1} (Jia et al.,
583 2020), but our results show NAG activity decreased at the high N deposition level, i.e. at N input
584 rates about an order of magnitude lower than that published threshold. This finding indicates that
585 soil microbial communities are sensitive to external N supplied at rates much lower than those
586 typically applied in N-fertilization studies (Averill et al., 2018), suggesting a low critical N load
587 to alter soil C-N dynamics. Although the reason for this large difference in thresholds is not
588 known, plants and soil microbes take up a small fraction of applied fertilizer-N because their net
589 sink rates are likely saturated (Lovett & Goodale, 2011). In contrast, in most regions of the
590 world, N deposition rates are lower than agricultural fertilization rates and consistent over time,
591 allowing for N accumulation in ecosystems. Future work should discern the quantity of
592 anthropogenic N required to alter competition for N between microbial heterotrophs and
593 nitrifiers and explicitly test microbial competition with measures of gross N transformation rates
594 across ecosystems.

595

596 *Spatiotemporal dynamics of microbial competition for N*

597 Despite a reduction in N deposition related to COVID-19 restrictions, there were no
598 major differences in net N transformation rates between 2020 and 2021. Soil C did not control
599 net N transformation rates nor $f_{\text{nitrified}}$ in 2021 at sites with intermediate and high background
600 rates of N deposition, in contrast to H2 (Fig. 1). Instead, it appears that background N deposition
601 was a mediator of the N cycle. Our findings are supported by the few N-cessation field
602 experiments that document soil net N mineralization (Clark et al., 2009; O'Sullivan et al., 2011)
603 and nitrification rates (Stienstra et al., 1994) in previously fertilized treatments remaining higher
604 than rates in unfertilized treatments for at least 10 years. These findings, along with our results,
605 are evidence of microbial functional legacies in which contemporary microbial functions are
606 driven by previous environmental conditions (Crowther et al., 2019; Hawkes et al., 2020;
607 Hawkes & Keitt, 2015), or that high levels of N supply persisted. With higher N availability
608 from past N deposition, the cumulative amount of anthropogenic N, rather than annually
609 supplied N concentration, appears to mutually control $f_{\text{nitrified}}$ along with soil C. Therefore, a
610 short-term dip in N deposition does not decrease net N transformation rates and $f_{\text{nitrified}}$.
611 Consequently, soil microbial functions may not change in tandem with ongoing declines in N
612 availability across most unmanaged landscapes (Mason et al., 2022; McLauchlan et al., 2017).

613 If background N deposition modifies the influence of soil C on net N transformations,
614 legacies of elevated net N transformation rates and $f_{\text{nitrified}}$ could persist after a decrease in
615 anthropogenic N deposition. The recovery of ecosystem pools and processes from high N
616 availability likely occurs non-linearly and asynchronously (Gilliam et al., 2019) because plants
617 and soil microbes jointly drive this recovery (Nieland & Zeglin, 2024). For example, low C:N

ratio in SOM can support high rates of N mineralization after N fertilization ceases (Frankenberger & Abdelmagid, 1985; Manzoni et al., 2008), but lower NH_4^+ availability due to immobilization can reduce nitrification rates and $f_{\text{nitrified}}$ within five years after N fertilization stops (Nieland & Zeglin, 2024). Given that dry N deposition rates decreased across 2018-2020, it appears that three years of total dry N decline was not long enough to disrupt the role of background N deposition across North American ecosystems. Plants also retain high concentrations of N in their biomass that later serve as a substrate for N once plant litter turns over (Cotrufo et al., 2015; Lavallee et al., 2020). For example, over longer time scales, early-seral N_2-fixing trees can leave legacies of elevated soil N availability that persist for tens to hundreds of years (Perakis et al., 2011; Von Holle et al., 2013). Thus, the effects of high background N deposition on soil C, net N mineralization, and net nitrification relationships may depend on the magnitude and duration of N deposition in combination with ecosystem-specific characteristics, such as plant community composition.

Conclusions and implications

Our measurements of net N transformations, $f_{\text{nitrified}}$, and microbial biomass and function at 39 sites in 14 regions across the contiguous U.S. document that N deposition can disrupt the role of soil C as a gatekeeper of coupled net N transformations. As deposition supplied more N to soil pools, the relationship between net N mineralization and net nitrification rates ($f_{\text{nitrified}}$) weakened because heterotrophs and nitrifiers shifted their N source. However, background N deposition rates of previous years, instead of N deposition inputs during the years of observation, controlled soil microbial responses. This finding suggests previous N deposition has a stronger role in the contemporary N cycle than current deposition. While inherent ecosystem properties

such as differences in vegetation or soil characteristics affect how ecosystems respond to higher N availability, our findings suggest that background N deposition uniformly disrupts the relationship between soil C and net N transformations across different ecosystems and climates. The cumulative effect of N deposition attenuates how soil C controls coupled net N transformations by decoupling NH_4^+ availability from soil N mineralization, which persists even with short-term (1-2 year) dips in deposition. With N deposition generally declining across the U.S. and more widely across the globe, it is unknown how long the historical imprint of N deposition will alter the relationship between soil C and net N transformations and whether this legacy will vary across soil and ecosystem types. In the short-term, predictions of N transformations, N availability and N losses should account for both soil C content and regional N deposition.

Acknowledgements

We thank Cameron Chin, Gabriella Griffen, and Sabrina Sprague for laboratory assistance. We also thank the Stable Isotope Ecology Laboratory at the University of Georgia and personnel for soil C and N data. This work was supported by the University of Massachusetts Amherst. Authors were supported by National Science Foundation awards (DEB-1831944 for SEH, EAR-2045135 for SSP, and 1845417 for MSS) and Department of Energy Office of Biological and Environmental Research (DE-SC0020382 for SDA). Any use of trade, firm, or product names is for descriptive purposes only and does not imply endorsement by the US Government.

Table 1 | The best fitting model explaining net nitrification rates that excludes soil pH and soil C:N. Background rates of N deposition was included since the model fit improved with its inclusion (AIC, 188.0 < 193.6 when excluding N deposition). All fixed effects were modeled as continuous variables. Unstandardized coefficients are reported for estimates.

Parameter	Estimate	*t*	*P*
Net N mineralization rate	1.091	5.41	**< 0.001**
Soil C	-0.120	-2.31	**0.024**
Soil moisture	-5.128	-1.87	0.065
Mean historical N deposition	-0.345	-3.02	**0.004**
Net N mineralization rate × Soil moisture	-1.666	-3.32	**0.001**
Soil moisture × Mean N deposition	1.04	2.93	**0.005**

P-values less 0.05 are bolded.

Adjusted $R^2 = 0.379$

669 **Table 2 |** The best fitting soil characteristics model explaining net nitrification rates. All fixed
670 effects were modeled as continuous variables. Unstandardized coefficients are reported for
671 estimates.
672

Parameter	Estimate	*t*	*P*
Net N mineralization rate	0.241	0.38	0.703
Soil C	-0.040	-0.46	0.648
Soil moisture	5.873	3.12	**0.003**
Soil C:N	0.024	0.68	0.500
Soil pH	0.077	0.51	0.611
Net N mineralization rate × Soil C	0.155	2.56	**0.013**
Net N mineralization rate × Soil moisture	-1.152	-2.10	**0.040**
Net N mineralization rate × Soil C:N	-0.075	-3.32	**0.002**
Net N mineralization rate × Soil pH	0.186	2.86	**0.006**
Soil C × Soil moisture	-0.524	-2.34	**0.023**

673
674 *P*-values less 0.05 are bolded.
675 Adjusted $R^2 = 0.719$

Table 3 | The best fitting soil chemistry models. Ecosystem, N deposition (N dep), and climate fixed effects were all modeled as categorical variables.

Response	Model	*F*, *P*
Soil pH	~ Ecosystem + N dep + Climate + Ecosystem × N dep + Ecosystem × Climate	**Ecosystem: $F_{3, 57} = 30.12$, $P < 0.001$** **N dep: $F_{2, 57} = 3.41$, $P = 0.040$** Climate: $F_{1, 57} = 2.95$, $P = 0.091$ **Ecosystem × N dep: $F_{5, 57} = 2.88$, $P = 0.031$** **Ecosystem × Climate: $F_{1, 57} = 6.74$, $P = 0.012$**
Soil C†	~ Ecosystem + N dep + Ecosystem × N dep	**Ecosystem: $F_{3, 59} = 11.38$, $P < 0.001$** **N dep: $F_{2, 59} = 4.89$, $P = 0.011$** **Ecosystem × N dep: $F_{4, 59} = 3.63$, $P = 0.010$**
Soil N†	~ Ecosystem + N dep + Ecosystem × N dep	**Ecosystem: $F_{3, 59} = 3.73$, $P = 0.016$** N dep: $F_{2, 59} = 2.86$, $P = 0.065$ **Ecosystem × N dep: $F_{4, 59} = 6.35$, $P < 0.001$**
Soil C:N ratio†	~ Ecosystem + N dep	**Ecosystem: $F_{3, 63} = 22.08$, $P < 0.001$** **N dep: $F_{2, 63} = 4.49$, $P = 0.015$**
Soil moisture	~ Ecosystem + Time + Ecosystem × Time	**Ecosystem: $F_{3, 64} = 9.63$, $P < 0.001$** **Time: $F_{1, 64} = 47.02$, $P < 0.001$** **Ecosystem × Time: $F_{3, 64} = 3.29$, $P = 0.026$**

Fixed effects with *P*-values less 0.05 are bolded.

†Soil chemistry responses were log-transformed to meet normality assumptions.

Figures

Fig. 1 | Conceptual model of hypotheses. (Top panel) Under low N deposition (a), net nitrification and N mineralization rates are expected to couple ($f_{\text{nitrified}} = 1$) in low soil C conditions due to reduced competition for NH_4^+ between microbial heterotrophs and nitrifiers. In contrast, high soil C facilitates strong competition, resulting in NH_4^+-limitation for nitrifiers and decoupled net nitrification and N mineralization rates ($f_{\text{nitrified}} = 0$). As background N deposition increases (b), competition between microbial heterotrophs and nitrifiers for NH_4^+ weakens as nitrifiers can switch their source for NH_4^+ resulting in higher net nitrification rates in high C soils. (c) A short-term dip in N deposition because of a COVID-19 response to reduced vehicle emissions is predicted to decrease net nitrification rates, lowering $f_{\text{nitrified}}$, particularly for soils with high C content as heterotrophic immobilization increases.

Fig. 2 | Distribution of site locations and background total (wet + dry) N deposition. (a) Map of the contiguous United States showing the 14 regions and average background N deposition rates from 2013-2017. Shapes of the points correspond to background N deposition classification. (b) Interannual variability in background total N deposition rates from 2013-2017 across N deposition class ranks.

Fig. 3 | Coupled-decoupled relationships between net N transformations as related to (a) soil C and (b) background N deposition rates. Coupled net N transformations align closely to a 1:1 relationship between net nitrification and N mineralization rates ($f_{\text{nitrified}} = 1$). Decoupled net N transformations fall along the horizontal lines ($f_{\text{nitrified}} = 0$). $f_{\text{nitrified}}$ values greater than 1 indicate net nitrification rates were greater than net N mineralization rates. (c) The $f_{\text{nitrified}}$ values across

low and high soil C environments visualized as boxplots. The number of independent observations is 75 (n = 75).

Fig. 4 | Correlations between $f_{nitrified}$ and net N mineralization with functional assessments of soil microbial communities. $f_{nitrified}$ increased with (a) microbial enzymatic investment for C relative to N (BG:NAG ratio), an index of microbial N limitation (n = 74), but decreased with increasing (b) active microbial biomass (n = 78). The $f_{nitrified}$ correlations were not different among background N deposition classes. (c) The association between net N mineralization and active microbial biomass varied significantly with N deposition (n = 78). Net N mineralization rates correlated significantly with active microbial biomass at low N deposition (β = 0.640, P = 0.020), but not at intermediate (β = 0.085, P = 0.358) or high (β = -0.2878, P = 0.096) N deposition as indicated by the dotted linear regressions. Line colors correspond to the point colors reflecting background N classification.

Fig. 5 | The relationship of (a) net nitrification and (b) net N mineralization rates and microbial enzymatic investment for C relative to N (microbial N limitation as indicated by the BG:NAG ratio, where higher BG:NAG indicates greater microbial investment in C relative to N acquisition). Each point is the net N transformation rate for each site at a collection time (n = 74). The black lines show the correlations between the net N transformations and the microbial N limitation index.

Fig. 6 | Soil chemistry and microbial functional effects on $f_{nitrified}$ under (a) low, (b), intermediate, and (c) high N deposition. Paths in the SEM (χ^2 = 3.61, df = 3, P = 0.307; Fisher's

C = 5.12, df = 6, $P = 0.529$) include the standardized effect sizes (boxes) under the different N deposition classes with solid lines indicating significant relationships at the $^{*}P < 0.05$, $^{**}P < 0.01$, and $^{***}P < 0.001$ levels that are sized proportionally to the effect size for the 71 independent observations ($n = 71$). Dotted lines show the insignificant paths for each deposition classification. The correlated error between soil C and N was 0.876. (d) The calculated direct, indirect, and total effects of soil C on $f_{\text{nitrified}}$ at low, intermediate, and high N deposition.

Fig. 7 | Net N transformation rates in 2020 and 2021 collected at the resampled sites to assess temporal changes resulting from changes in N deposition from the COVID-19 pandemic ($n = 154$). (a) Net N mineralization rates were higher in 2021 than 2020 for the Mixed Forest - S. CT site. (b) Net nitrification rates varied significantly between 2020 and 2021 for some collection points for two sites. Points are the mean rates (± 1 standard error) at each time point separated by year. Asterisks above points in (b) indicate statistical differences between years at the time collection at the $^{**}P < 0.01$ and $^{***}P < 0.001$ thresholds.

741 **Fig. 1**

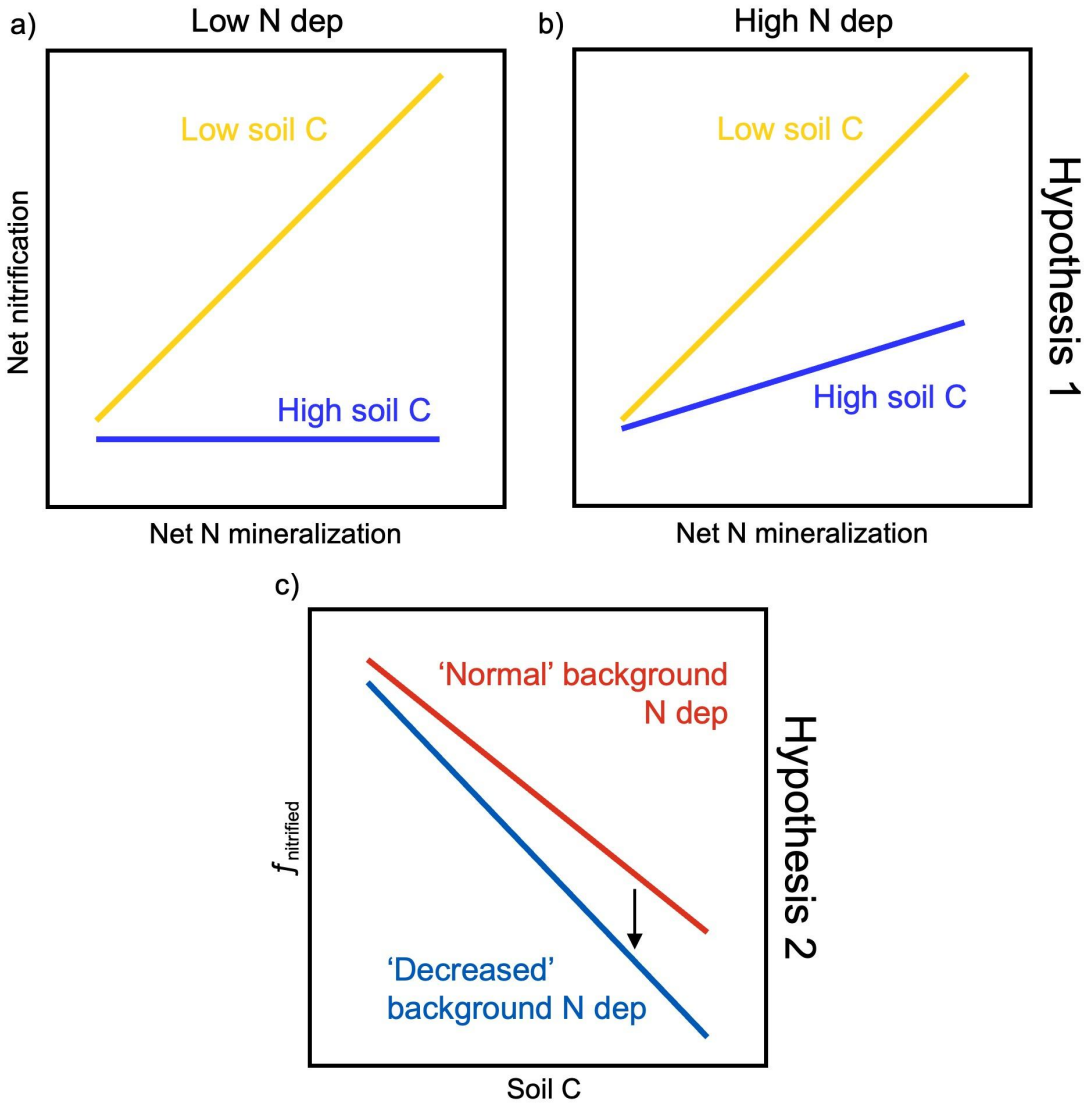

742

743

744 **Fig. 2**

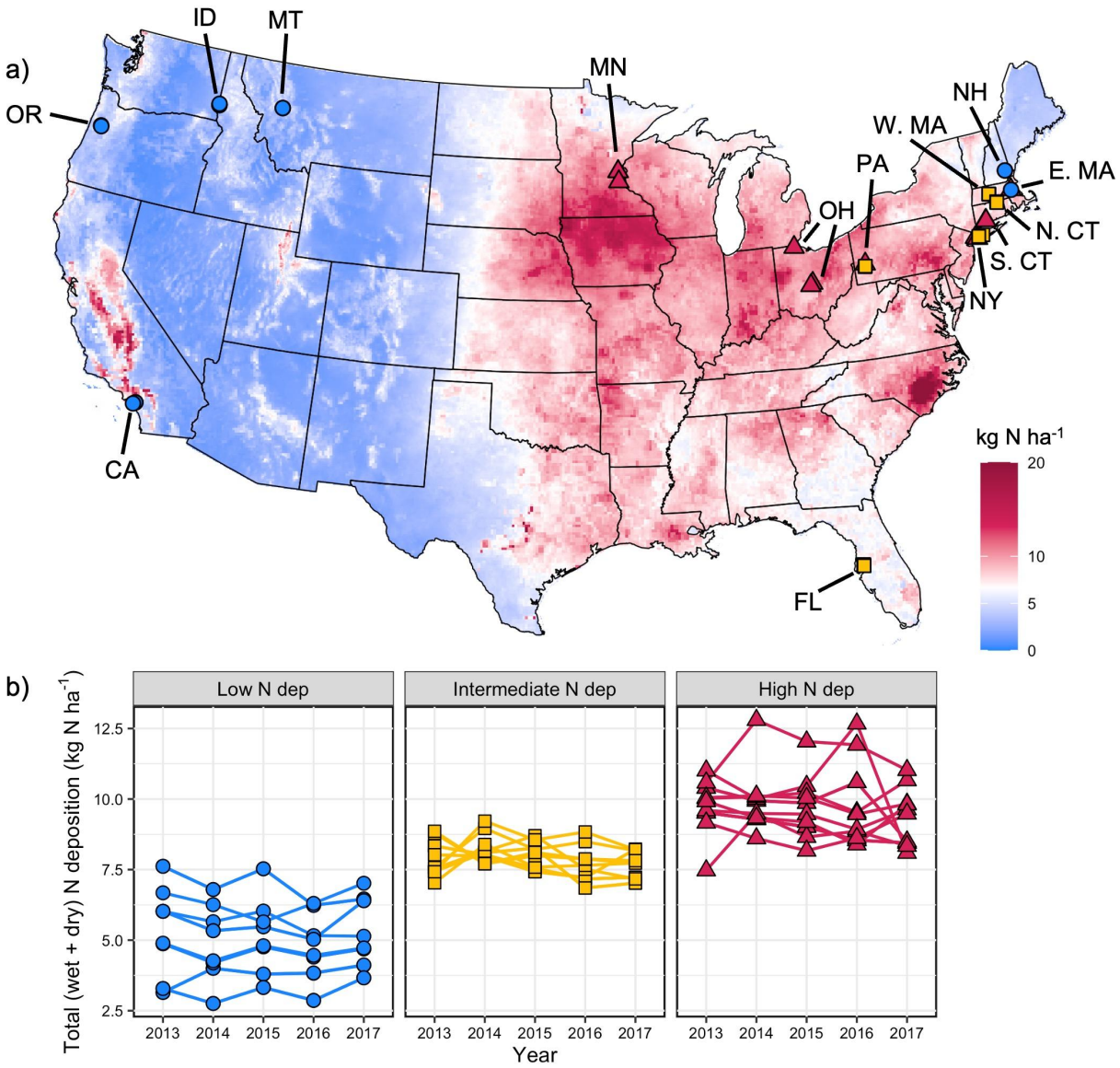

745

746

747 **Fig. 3**

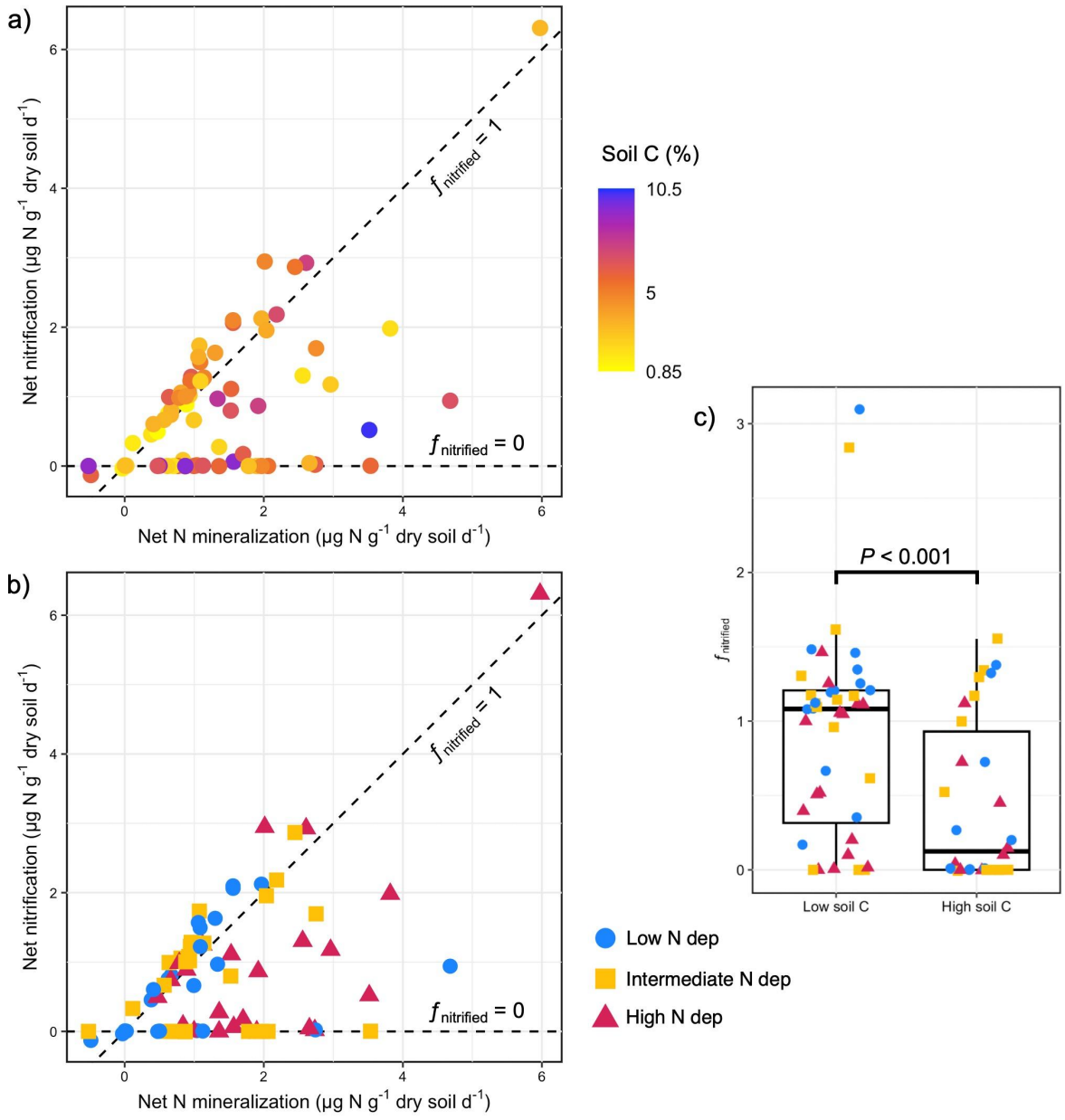

748

749

750 **Fig. 4**

751

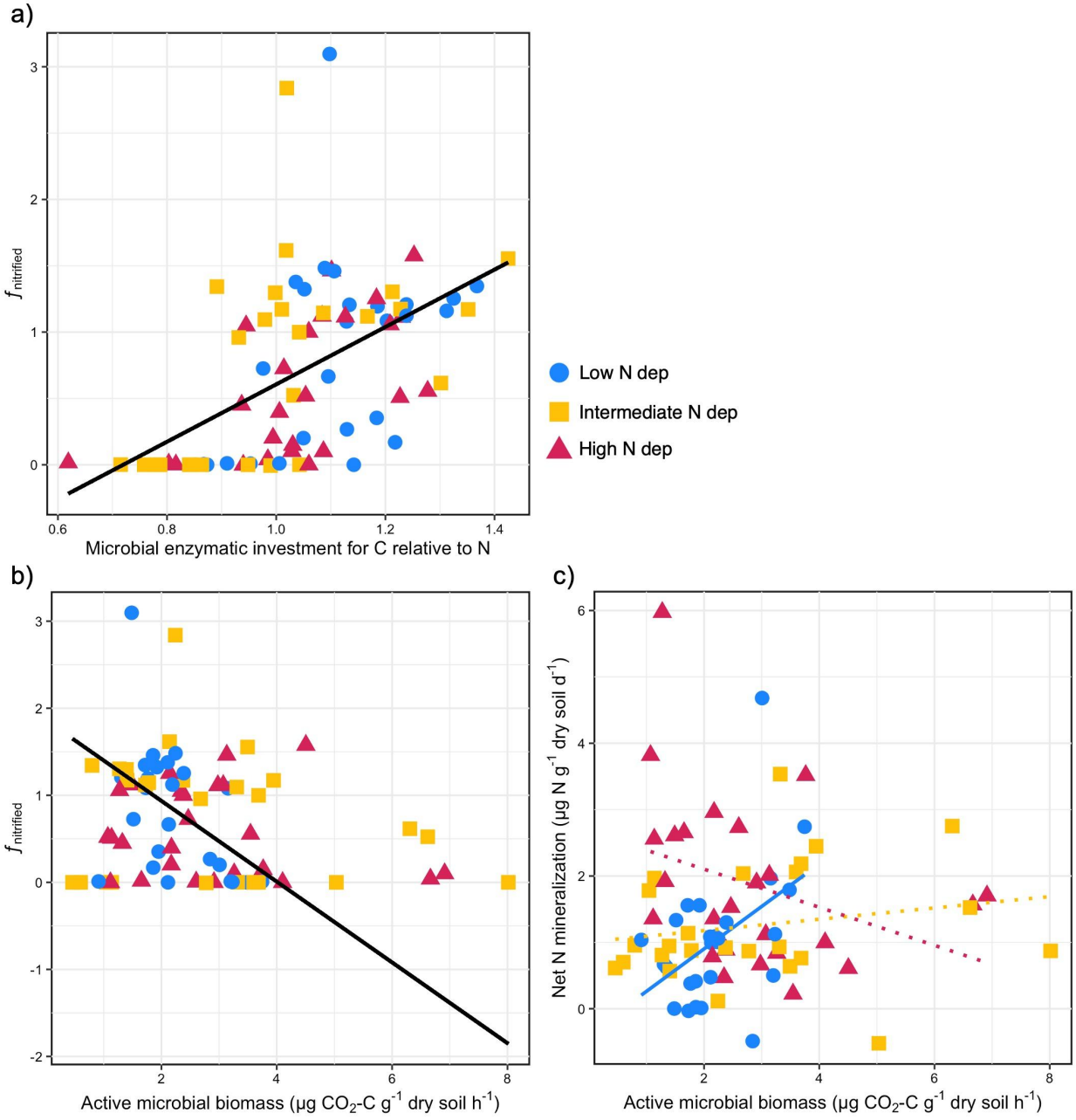

752

753 **Fig. 5**

754

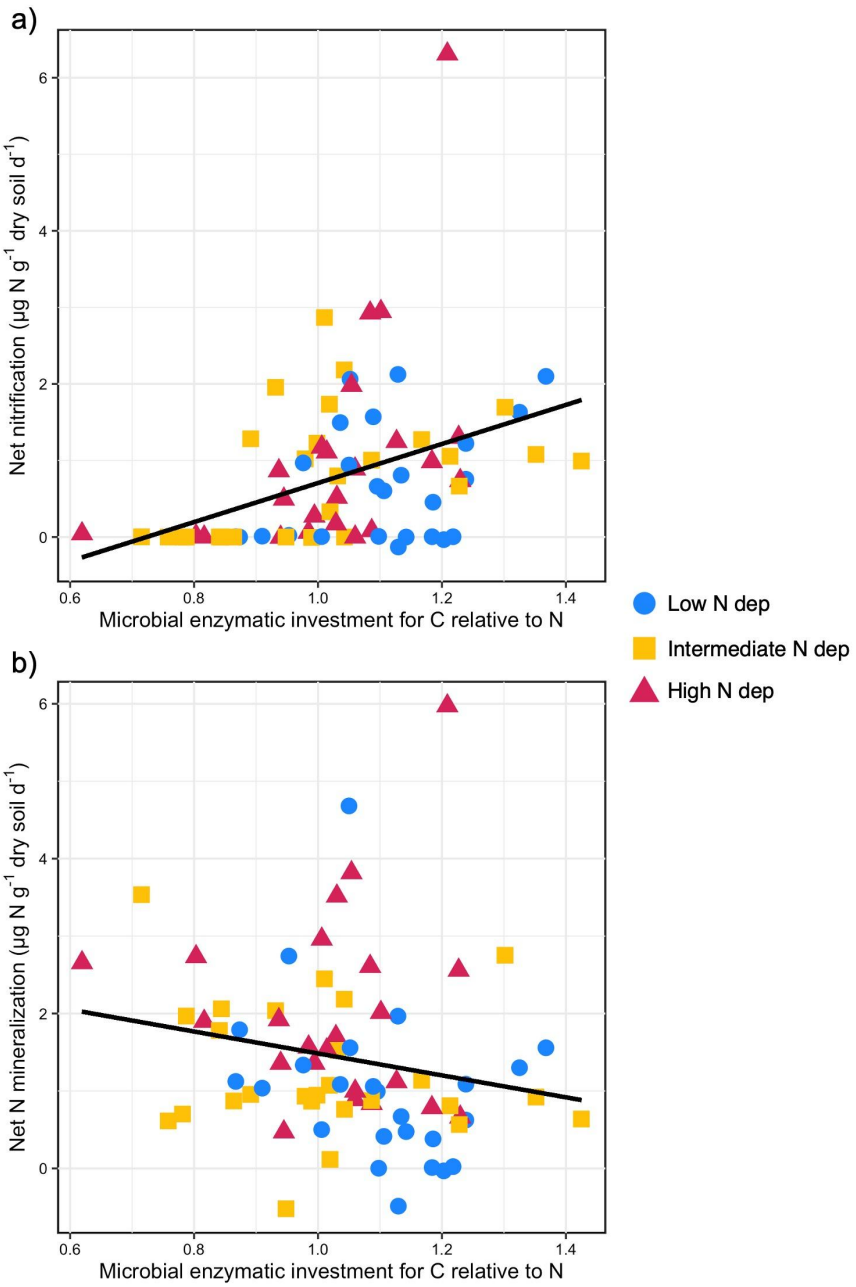
a)
Net nitrification (μg N g-1 dry soil d-1)
0
2
4
6
0.6
0.8
1.0
1.2
1.4
Microbial enzymatic investment for C relative to N
b)
Net N mineralization (μg N g-1 dry soil d-1)
0
2
4
6
0.6
0.8
1.0
1.2
1.4
Microbial enzymatic investment for C relative to N
Low N dep
Intermediate N dep
High N dep

755 **Fig. 6**

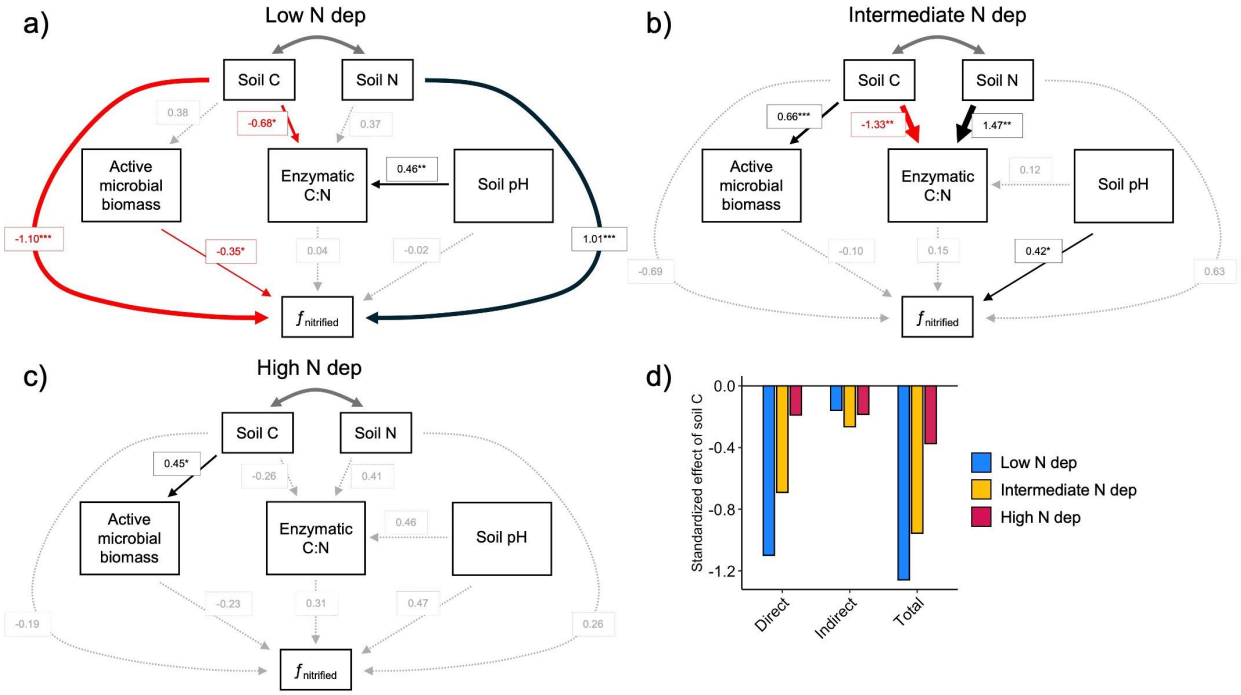
a)
Low N dep
Soil C
Soil N
Active microbial biomass
Enzymatic C:N
Soil pH
0.38
-0.68*
0.37
0.46**
-1.10***
-0.35*
0.04
-0.02
1.01***
$f_{nitrified}$
b)
Intermediate N dep
Soil C
Soil N
Active microbial biomass
Enzymatic C:N
Soil pH
0.66***
-1.33**
1.47**
0.12
-0.69
-0.10
0.15
0.42*
0.63
$f_{nitrified}$
c)
High N dep
Soil C
Soil N
Active microbial biomass
Enzymatic C:N
Soil pH
0.45*
-0.26
0.41
0.46
-0.19
-0.23
0.31
0.47
0.26
$f_{nitrified}$
d)
Standardized effect of soil C
0.0
-0.4
-0.8
-1.2
Direct
Indirect
Total
Low N dep
Intermediate N dep
High N dep

756

757 **Fig. 7**

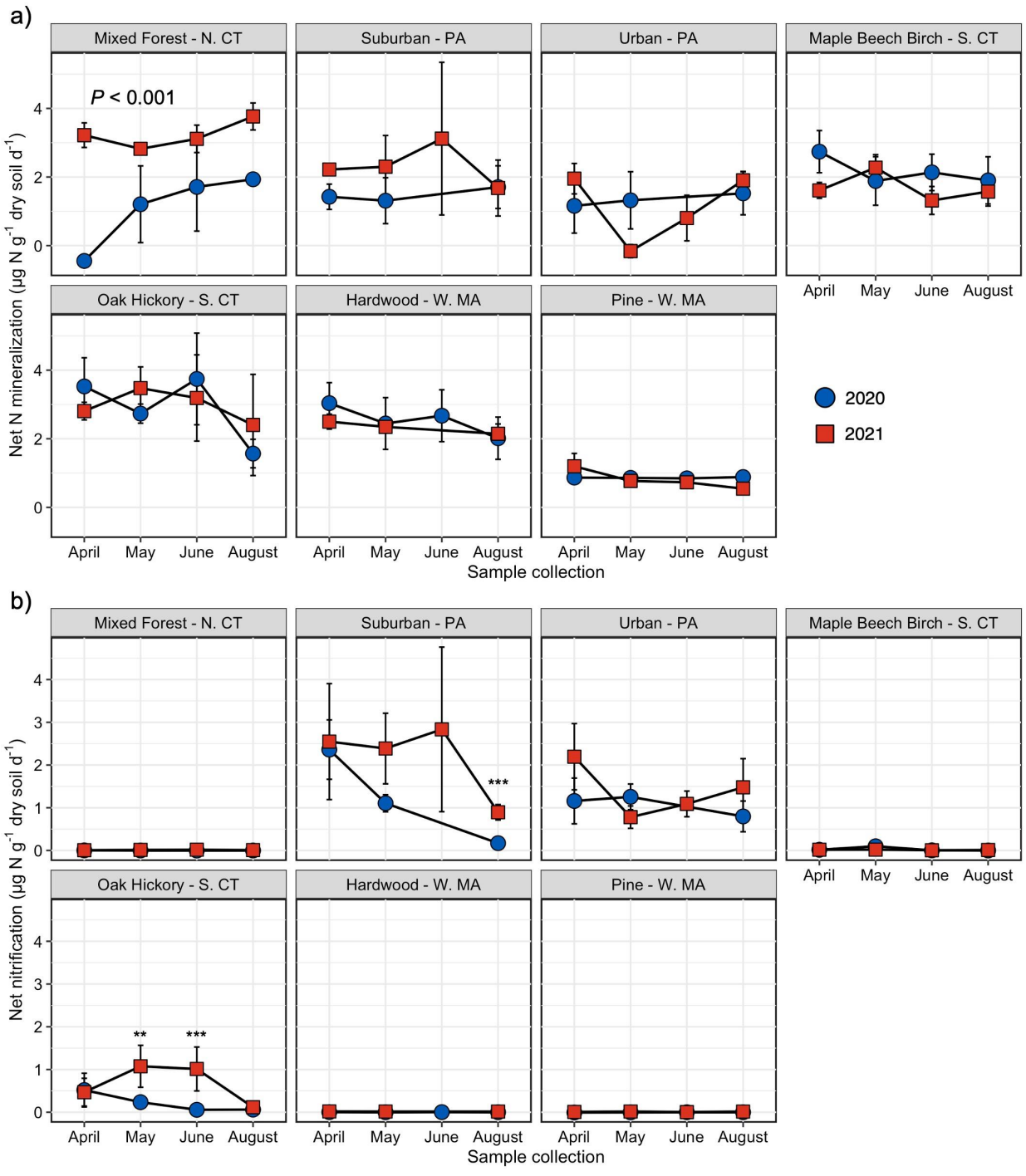
a)
Mixed Forest - N. CT
Suburban - PA
Urban - PA
Maple Beech Birch - S. CT
Oak Hickory - S. CT
Hardwood - W. MA
Pine - W. MA
P < 0.001
Net N mineralization (µg N g-1 dry soil d-1)
April
May
June
August
Sample collection
2020
2021
b)
Net nitrification (µg N g-1 dry soil d-1)
***
**
***

758

References

Aber, J., McDowell, W., Nadelhoffer, K., Magill, A., Berntson, G., Kamakea, M., McNulty, S., Currie, W., Rustad, L., & Fernandez, I. (1998). Nitrogen Saturation in Temperate Forest Ecosystems. *BioScience*, *48*(11), 921–934. https://doi.org/10.2307/1313296

Ackerman, D., Millet, D. B., & Chen, X. (2019). Global Estimates of Inorganic Nitrogen Deposition Across Four Decades. *Global Biogeochemical Cycles*, *33*(1), 100–107. https://doi.org/10.1029/2018GB005990

Ajwa, H. A., Dell, C. J., & Rice, C. W. (1999). Changes in enzyme activities and microbial biomass of tallgrass prairie soil as related to burning and nitrogen fertilization. *Soil Biology and Biochemistry*, *31*(5), 769–777. https://doi.org/10.1016/S0038-0717(98)00177-1

Alfano, V., & Ercolano, S. (2020). The Efficacy of Lockdown Against COVID-19: A Cross-Country Panel Analysis. *Applied Health Economics and Health Policy*, *18*(4), 509–517. https://doi.org/10.1007/s40258-020-00596-3

Allen, R. G., Pereira, L. S., Raes, D., & Smith, M. (1999). *Crop Evapotranspiration. Guidelines for Computing Crop Water Requirements* (56; FAO Irrigation and Drainage Paper, p. 300). United Nations – FAO.

Allen, S. E. (Ed.). (1974). *Chemical analysis of ecological materials*. Blackwell Scientific.

Allison, S. D., & Vitousek, P. M. (2005). Responses of extracellular enzymes to simple and complex nutrient inputs. *Soil Biology and Biochemistry*, *37*(5), 937–944. https://doi.org/10.1016/j.soilbio.2004.09.014

780 Anderson, J. P. E., & Domsch, K. H. (1978). A physiological method for the quantitative
781 measurement of microbial biomass in soils. *Soil Biology and Biochemistry*, *10*(3), 215–
782 221. https://doi.org/10.1016/0038-0717(78)90099-8
783 Averill, C., Dietze, M. C., & Bhatnagar, J. M. (2018). Continental-scale nitrogen pollution is
784 shifting forest mycorrhizal associations and soil carbon stocks. *Global Change Biology*,
785 *24*(10), 4544–4553. https://doi.org/10.1111/gcb.14368
786 Bates, D., Mächler, M., Bolker, B., & Walker, S. (2015). Fitting Linear Mixed-Effects Models
787 Using lme4. *Journal of Statistical Software*, *67*(1). https://doi.org/10.18637/jss.v067.i01
788 Benish, S. E., Bash, J. O., Foley, K. M., Appel, K. W., Hogrefe, C., Gilliam, R., & Pouliot, G.
789 (2022). Long-term regional trends of nitrogen and sulfur deposition in the United States
790 from 2002 to 2017. *Atmospheric Chemistry and Physics*, *22*(19), 12749–12767.
791 https://doi.org/10.5194/acp-22-12749-2022
792 Berman, J. D., & Ebisu, K. (2020). Changes in U.S. air pollution during the COVID-19
793 pandemic. *Science of The Total Environment*, *739*, 139864.
794 https://doi.org/10.1016/j.scitotenv.2020.139864
795 Bettez, N. D., & Groffman, P. M. (2013). Nitrogen Deposition in and near an Urban Ecosystem.
796 *Environmental Science & Technology*, *47*(11), 6047–6051.
797 https://doi.org/10.1021/es400664b
798 Bowden, R. D., Wurzbacher, S. J., Washko, S. E., Wind, L., Rice, A. M., Coble, A. E., Baldauf,
799 N., Johnson, B., Wang, J., Simpson, M., & Lajtha, K. (2019). Long-term Nitrogen
800 Addition Decreases Organic Matter Decomposition and Increases Forest Soil Carbon.
801 *Soil Science Society of America Journal*, *83*(S1).
802 https://doi.org/10.2136/sssaj2018.08.0293

Bradford, M. A., Davies, C. A., Frey, S. D., Maddox, T. R., Melillo, J. M., Mohan, J. E., Reynolds, J. F., Treseder, K. K., & Wallenstein, M. D. (2008). Thermal adaptation of soil microbial respiration to elevated temperature. *Ecology Letters*, *11*(12), 1316–1327. https://doi.org/10.1111/j.1461-0248.2008.01251.x

Bradford, M. A., Fierer, N., & Reynolds, J. F. (2008). Soil carbon stocks in experimental mesocosms are dependent on the rate of labile carbon, nitrogen and phosphorus inputs to soils. *Functional Ecology*, *22*(6), 964–974. https://doi.org/10.1111/j.1365-2435.2008.01404.x

Burns, R. G. (1982). Enzyme activity in soil: Location and a possible role in microbial ecology. *Soil Biology and Biochemistry*, *14*(5), 423–427. https://doi.org/10.1016/0038-0717(82)90099-2

Carson, C. M., Jumpponen, A., Blair, J. M., & Zeglin, L. H. (2019). Soil fungal community changes in response to long-term fire cessation and N fertilization in tallgrass prairie. *Fungal Ecology*, *41*, 45–55. https://doi.org/10.1016/j.funeco.2019.03.002

Chróst, R. J. (1991). *Environmental Control of the Synthesis and Activity of Aquatic Microbial Ectoenzymes* (pp. 29–59). https://doi.org/10.1007/978-1-4612-3090-8_3

Clark, C. M., Hobbie, S. E., Venterea, R., & Tilman, D. (2009). Long-lasting effects on nitrogen cycling 12 years after treatments cease despite minimal long-term nitrogen retention. *Global Change Biology*, *15*(7), 1755–1766. https://doi.org/10.1111/j.1365-2486.2008.01811.x

Cleveland, C. C., & Liptzin, D. (2007). C:N:P stoichiometry in soil: Is there a “Redfield ratio” for the microbial biomass? *Biogeochemistry*, *85*(3), 235–252. https://doi.org/10.1007/s10533-007-9132-0

826 Cotrufo, M. F., Soong, J. L., Horton, A. J., Campbell, E. E., Haddix, M. L., Wall, D. H., &
827 Parton, W. J. (2015). Formation of soil organic matter via biochemical and physical
828 pathways of litter mass loss. *Nature Geoscience*, *8*(10), 776–779.
829 https://doi.org/10.1038/ngeo2520
830 Craine, J. M., Morrow, C., Fierer, N., Craine, J. M., Morrow, C., & Fierer, N. (2007). Microbial
831 Nitrogen Limitation Increases Decomposition. *Ecology*, *88*(8), 2105–2113.
832 Crowther, T. W., van den Hoogen, J., Wan, J., Mayes, M. A., Keiser, A. D., Mo, L., Averill, C.,
833 & Maynard, D. S. (2019). The global soil community and its influence on
834 biogeochemistry. *Science*, *365*(6455), eaav0550. https://doi.org/10.1126/science.aav0550
835 Dijkstra, P., LaViolette, C. M., Coyle, J. S., Doucett, R. R., Schwartz, E., Hart, S. C., & Hungate,
836 B. A. (2008). ^{15} N enrichment as an integrator of the effects of C and N on microbial
837 metabolism and ecosystem function. *Ecology Letters*, *11*(4), 389–397.
838 https://doi.org/10.1111/j.1461-0248.2008.01154.x
839 Edwards, I. P., Zak, D. R., Kellner, H., Eisenlord, S. D., & Pregitzer, K. S. (2011). Simulated
840 Atmospheric N Deposition Alters Fungal Community Composition and Suppresses
841 Ligninolytic Gene Expression in a Northern Hardwood Forest. *PLoS ONE*, *6*(6), e20421.
842 https://doi.org/10.1371/journal.pone.0020421
843 Elrys, A. S., Wang, J., Metwally, M. A. S., Cheng, Y., Zhang, J., Cai, Z., Chang, S. X., &
844 Müller, C. (2021). Global gross nitrification rates are dominantly driven by soil carbon-
845 to-nitrogen stoichiometry and total nitrogen. *Global Change Biology*, *27*(24), 6512–6524.
846 https://doi.org/10.1111/gcb.15883

847 Fierer, N., Wood, S. A., & Bueno De Mesquita, C. P. (2021). How microbes can, and cannot, be
848 used to assess soil health. *Soil Biology and Biochemistry*, *153*, 108111.
849 https://doi.org/10.1016/j.soilbio.2020.108111
850 Fixen, P. E., & West, F. B. (2002). Nitrogen Fertilizers: Meeting Contemporary Challenges.
851 *AMBIO: A Journal of the Human Environment*, *31*(2), 169–176.
852 https://doi.org/10.1579/0044-7447-31.2.169
853 Frankenberger, W. T., & Abdelmagid, H. M. (1985). Kinetic parameters of nitrogen
854 mineralization rates of leguminous crops incorporated into soil. *Plant and Soil*, *87*(2),
855 257–271.
856 Frey, S. D., Knorr, M., Parrent, J. L., & Simpson, R. T. (2004). Chronic nitrogen enrichment
857 affects the structure and function of the soil microbial community in temperate hardwood
858 and pine forests. *Forest Ecology and Management*, *196*(1), 159–171.
859 https://doi.org/10.1016/j.foreco.2004.03.018
860 Frey, S. D., Ollinger, S., Nadelhoffer, K., Bowden, R., Brzostek, E., Burton, A., Caldwell, B. A.,
861 Crow, S., Goodale, C. L., Grandy, A. S., Finzi, A., Kramer, M. G., Lajtha, K., LeMoine,
862 J., Martin, M., McDowell, W. H., Minocha, R., Sadowsky, J. J., Templer, P. H., &
863 Wickings, K. (2014). Chronic nitrogen additions suppress decomposition and sequester
864 soil carbon in temperate forests. *Biogeochemistry*, *121*(2), 305–316.
865 https://doi.org/10.1007/s10533-014-0004-0
866 Frijlink, M. J., Abee, T., Laanbroek, H. J., De Boer, W., & Konings, W. N. (1992). The
867 bioenergetics of ammonia and hydroxylamine oxidation in Nitrosomonas europaea at
868 acid and alkaline pH. *Archives of Microbiology*, *157*(2), 194–199.
869 https://doi.org/10.1007/BF00245290

García-Ruiz, R., Ochoa, V., Hinojosa, M. B., & Carreira, J. A. (2008). Suitability of enzyme activities for the monitoring of soil quality improvement in organic agricultural systems. *Soil Biology and Biochemistry*, *40*(9), 2137–2145. https://doi.org/10.1016/j.soilbio.2008.03.023

Garten, C. T., Iversen, C. M., & Norby, R. J. (2011). Litterfall ^{15} N abundance indicates declining soil nitrogen availability in a free-air CO_2 enrichment experiment. *Ecology*, *92*(1), 133–139. https://doi.org/10.1890/10-0293.1

German, D. P., Weintraub, M. N., Grandy, A. S., Lauber, C. L., Rinkes, Z. L., & Allison, S. D. (2011). Optimization of hydrolytic and oxidative enzyme methods for ecosystem studies. *Soil Biology and Biochemistry*, *43*(7), 1387–1397. https://doi.org/10.1016/j.soilbio.2011.03.017

Gill, A. L., Grinder, R. M., See, C. R., Chapin, F. S., DeLancey, L. C., Fisk, M. C., Groffman, P. M., Harms, T., Hobbie, S. E., Knoepp, J. D., Knops, J. M. H., Mack, M., Reich, P. B., & Keiser, A. D. (2023). Soil carbon availability decouples net nitrogen mineralization and net nitrification across United States Long Term Ecological Research sites. *Biogeochemistry*, *162*(1), 13–24. https://doi.org/10.1007/s10533-022-01011-w

Gilliam, F. S., Burns, D. A., Driscoll, C. T., Frey, S. D., Lovett, G. M., & Watmough, S. A. (2019). Decreased atmospheric nitrogen deposition in eastern North America: Predicted responses of forest ecosystems. *Environmental Pollution*, *244*, 560–574. https://doi.org/10.1016/j.envpol.2018.09.135

Groffman, P. M., Driscoll, C. T., Durán, J., Campbell, J. L., Christenson, L. M., Fahey, T. J., Fisk, M. C., Fuss, C., Likens, G. E., Lovett, G., Rustad, L., & Templer, P. H. (2018).

Nitrogen oligotrophication in northern hardwood forests. *Biogeochemistry*, *141*(3), 523–539. https://doi.org/10.1007/s10533-018-0445-y

Gruber, N., & Galloway, J. N. (2008). An Earth-system perspective of the global nitrogen cycle. *Nature*, *451*, 293–296. https://doi.org/10.1038/nature06592

Hart, S. C., Nason, G. E., Myrold, D. D., & Perry, D. A. (1994). Dynamics of Gross Nitrogen Transformations in an Old-Growth Forest: The Carbon Connection. *Ecology*, *75*(4), 880–891. https://doi.org/10.2307/1939413

Hawkes, C. V., & Keitt, T. H. (2015). Resilience vs. Historical contingency in microbial responses to environmental change. *Ecology Letters*, *18*(7), 612–625. https://doi.org/10.1111/ele.12451

Hawkes, C. V., Shinada, M., & Kivlin, S. N. (2020). Historical climate legacies on soil respiration persist despite extreme changes in rainfall. *Soil Biology and Biochemistry*, *143*, 107752. https://doi.org/10.1016/j.soilbio.2020.107752

Hobbie, S. E. (2015). Plant species effects on nutrient cycling: Revisiting litter feedbacks. *Trends in Ecology & Evolution*, *30*(6), 357–363. https://doi.org/10.1016/j.tree.2015.03.015

Holland, E. A., Braswell, B. H., Sulzman, J., & Lamarque, J.-F. (2005). NITROGEN DEPOSITION ONTO THE UNITED STATES AND WESTERN EUROPE: SYNTHESIS OF OBSERVATIONS AND MODELS. *Ecological Applications*, *15*(1), 38–57. https://doi.org/10.1890/03-5162

Hood-Nowotny, R., Hinko-Najera Umana, N., Inselbacher, E., & Oswald- Lachouani Wanek Wolfgang, P. (2010). Alternative Methods for Measuring Inorganic, Organic, and Total Dissolved Nitrogen in Soil. *Soil Science Society of America Journal*, *74*(3), 1018–1027. https://doi.org/10.2136/sssaj2009.0389

Jia, X., Zhong, Y., Liu, J., Zhu, G., Shangguan, Z., & Yan, W. (2020). Effects of nitrogen enrichment on soil microbial characteristics: From biomass to enzyme activities. *Geoderma*, *366*, 114256. https://doi.org/10.1016/j.geoderma.2020.114256

Jian, S., Li, J., Chen, J., Wang, G., Mayes, M. A., Dzantor, K. E., Hui, D., & Luo, Y. (2016). Soil extracellular enzyme activities, soil carbon and nitrogen storage under nitrogen fertilization: A meta-analysis. *Soil Biology and Biochemistry*, *101*, 32–43. https://doi.org/10.1016/j.soilbio.2016.07.003

Keiser, A. D., Knoepp, J. D., & Bradford, M. A. (2016). Disturbance Decouples Biogeochemical Cycles Across Forests of the Southeastern US. *Ecosystems*, *19*(1), 50–61. https://doi.org/10.1007/s10021-015-9917-2

Keiser, A. D., Smith, M., Bell, S., & Hofmockel, K. S. (2019). Peatland microbial community response to altered climate tempered by nutrient availability. *Soil Biology and Biochemistry*, *137*, 107561. https://doi.org/10.1016/j.soilbio.2019.107561

Keller, A. B., Borer, E. T., Collins, S. L., DeLancey, L. C., Fay, P. A., Hofmockel, K. S., Leakey, A. D. B., Mayes, M. A., Seabloom, E. W., Walter, C. A., Wang, Y., Zhao, Q., & Hobbie, S. E. (2022). Soil carbon stocks in temperate grasslands differ strongly across sites but are insensitive to decade-long fertilization. *Global Change Biology*, *28*(4), 1659–1677. https://doi.org/10.1111/gcb.15988

Kemmitt, S., Wright, D., Goulding, K., & Jones, D. (2006). pH regulation of carbon and nitrogen dynamics in two agricultural soils. *Soil Biology and Biochemistry*, *38*(5), 898–911. https://doi.org/10.1016/j.soilbio.2005.08.006

Knapp, A. K., Beier, C., Briske, D. D., Classen, A. T., Luo, Y., Reichstein, M., Smith, M. D., Smith, S. D., Bell, J. E., Fay, P. A., Heisler, J. L., Leavitt, S. W., Sherry, R., Smith, B., &

Weng, E. (2008). Consequences of More Extreme Precipitation Regimes for Terrestrial Ecosystems. *BioScience*, *58*(9), 811–821. https://doi.org/10.1641/B580908

Knorr, M., Frey, S. D., & Curtis, P. S. (2005). NITROGEN ADDITIONS AND LITTER DECOMPOSITION: A META-ANALYSIS. *Ecology*, *86*(12), 3252–3257. https://doi.org/10.1890/05-0150

Kuznetsova, A., Brockhoff, P. B., & Christensen, R. H. B. (2017). lmerTest Package: Tests in Linear Mixed Effects Models. *Journal of Statistical Software*, *82*(13), 1–26. https://doi.org/10.18637/jss.v082.i13

Lamarque, J.-F., Dentener, F., McConnell, J., Ro, C.-U., Shaw, M., Vet, R., Bergmann, D., Cameron-Smith, P., Dalsoren, S., Doherty, R., Faluvegi, G., Ghan, S. J., Josse, B., Lee, Y. H., MacKenzie, I. A., Plummer, D., Shindell, D. T., Skeie, R. B., Stevenson, D. S., … Nolan, M. (2013). Multi-model mean nitrogen and sulfur deposition from the Atmospheric Chemistry and Climate Model Intercomparison Project (ACCMIP): Evaluation of historical and projected future changes. *Atmospheric Chemistry and Physics*, *13*(16), 7997–8018. https://doi.org/10.5194/acp-13-7997-2013

Lavallee, J. M., Soong, J. L., & Cotrufo, M. F. (2020). Conceptualizing soil organic matter into particulate and mineral-associated forms to address global change in the 21st century. *Global Change Biology*, *26*(1), 261–273. https://doi.org/10.1111/gcb.14859

Le Quéré, C., Jackson, R. B., Jones, M. W., Smith, A. J. P., Abernethy, S., Andrew, R. M., De-Gol, A. J., Willis, D. R., Shan, Y., Canadell, J. G., Friedlingstein, P., Creutzig, F., & Peters, G. P. (2020). Temporary reduction in daily global CO2 emissions during the COVID-19 forced confinement. *Nature Climate Change*, *10*(7), 647–653. https://doi.org/10.1038/s41558-020-0797-x

961 Lefcheck, J. S. (2016). PIECEWISESEM: Piecewise structural equation modelling in R for ecology,
962 evolution, and systematics. *Methods in Ecology and Evolution*, *7*(5), 573–579.
963 https://doi.org/10.1111/2041-210X.12512
964 Li, X., Li, Z., Zhang, X., Xia, L., Zhang, W., Ma, Q., & He, H. (2020). Disentangling
965 immobilization of nitrate by fungi and bacteria in soil to plant residue amendment.
966 *Geoderma*, *374*, 114450. https://doi.org/10.1016/j.geoderma.2020.114450
967 Li, Y., Schichtel, B. A., Walker, J. T., Schwede, D. B., Chen, X., Lehmann, C. M. B., Puchalski,
968 M. A., Gay, D. A., & Collett, J. L. (2016). Increasing importance of deposition of
969 reduced nitrogen in the United States. *Proceedings of the National Academy of Sciences*,
970 *113*(21), 5874–5879. https://doi.org/10.1073/pnas.1525736113
971 Li, Z., Zeng, Z., Song, Z., Wang, F., Tian, D., Mi, W., Huang, X., Wang, J., Song, L., Yang, Z.,
972 Wang, J., Feng, H., Jiang, L., Chen, Y., Luo, Y., & Niu, S. (2021). Vital roles of soil
973 microbes in driving terrestrial nitrogen immobilization. *Global Change Biology*, *27*(9),
974 1848–1858. https://doi.org/10.1111/gcb.15552
975 Linn, D. M., & Doran, J. W. (1984). Effect of Water-Filled Pore Space on Carbon Dioxide and
976 Nitrous Oxide Production in Tilled and Nontilled Soils. *Soil Science Society of America*
977 *Journal*, *48*(6), 1267–1272. https://doi.org/10.2136/sssaj1984.03615995004800060013x
978 Liu, L., Xu, W., Lu, X., Zhong, B., Guo, Y., Lu, X., Zhao, Y., He, W., Wang, S., Zhang, X., Liu,
979 X., & Vitousek, P. (2022). Exploring global changes in agricultural ammonia emissions
980 and their contribution to nitrogen deposition since 1980. *Proceedings of the National*
981 *Academy of Sciences*, *119*(14), e2121998119. https://doi.org/10.1073/pnas.2121998119

Liu, Z., & Stern, R. (2021). Quantifying the Traffic Impacts of the COVID-19 Shutdown. *Journal of Transportation Engineering, Part A: Systems*, *147*(5), 04021014. https://doi.org/10.1061/JTEPBS.0000527

Long, J. A. (2019). *interactions: Comprehensive, User-Friendly Toolkit for Probing Interactions* (p. 1.2.0) [Dataset]. https://doi.org/10.32614/CRAN.package.interactions

Lovett, G. M., & Goodale, C. L. (2011). A New Conceptual Model of Nitrogen Saturation Based on Experimental Nitrogen Addition to an Oak Forest. *Ecosystems*, *14*(4), 615–631. https://doi.org/10.1007/s10021-011-9432-z

Manzoni, S., Jackson, R. B., Trofymow, J. A., & Porporato, A. (2008). The Global Stoichiometry of Litter Nitrogen Mineralization. *Science*, *321*(5889), 684–686. https://doi.org/10.1126/science.1159792

Mason, R. E., Craine, J. M., Lany, N. K., Jonard, M., Ollinger, S. V., Groffman, P. M., Fulweiler, R. W., Angerer, J., Read, Q. D., Reich, P. B., Templer, P. H., & Elmore, A. J. (2022). Evidence, causes, and consequences of declining nitrogen availability in terrestrial ecosystems. *Science*, *376*(6590), eabh3767. https://doi.org/10.1126/science.abh3767

McLauchlan, K. K., Gerhart, L. M., Battles, J. J., Craine, J. M., Elmore, A. J., Higuera, P. E., Mack, M. C., McNeil, B. E., Nelson, D. M., Pederson, N., & Perakis, S. S. (2017). Centennial-scale reductions in nitrogen availability in temperate forests of the United States. *Scientific Reports*, *7*(1), 7856. https://doi.org/10.1038/s41598-017-08170-z

McLauchlan, K. K., & Hobbie, S. E. (2004). Comparison of Labile Soil Organic Matter Fractionation Techniques. *Soil Science Society of America Journal*, *68*(5), 1616–1625. https://doi.org/10.2136/sssaj2004.1616

Melillo, J. M., Aber, J. D., Linkins, A. E., Ricca, A., Fry, B., & Nadelhoffer, K. J. (1989). Carbon and nitrogen dynamics along the decay continuum: Plant litter to soil organic matter. *Plant and Soil*, *115*(2), 189–198. https://doi.org/10.1007/BF02202587

Nieland, M. A., Carson, C. M., Floyd, V., & Zeglin, L. H. (2024). Product-inhibition feedbacks, not microbial population level tradeoffs or soil pH, regulate decomposition potential under nutrient eutrophication. *Soil Biology and Biochemistry*, *189*, 109247. https://doi.org/10.1016/j.soilbio.2023.109247

Nieland, M. A., Moley, P., Hanschu, J., & Zeglin, L. H. (2021). Differential Resilience of Soil Microbes and Ecosystem Functions Following Cessation of Long-Term Fertilization. *Ecosystems*, *24*(8), 2042–2060. https://doi.org/10.1007/s10021-021-00633-9

Nieland, M. A., & Zeglin, L. H. (2024). Plant and microbial feedbacks maintain soil nitrogen legacies in burned and unburned grasslands. *Journal of Ecology*, 1365-2745.14386. https://doi.org/10.1111/1365-2745.14386

Norby, R. J., Warren, J. M., Iversen, C. M., Medlyn, B. E., & McMurtrie, R. E. (2010). CO_2 enhancement of forest productivity constrained by limited nitrogen availability. *Proceedings of the National Academy of Sciences*, *107*(45), 19368–19373. https://doi.org/10.1073/pnas.1006463107

Olff, H., Aerts, R., Bobbink, R., Cornelissen, J. H. C., Erisman, J. W., Galloway, J. N., Stevens, C. J., Sutton, M. A., De Vries, F. T., Wamelink, G. W. W., & Wardle, D. A. (2022). Explanations for nitrogen decline. *Science*, *376*(6598), 1169–1170. https://doi.org/10.1126/science.abq7575

O'Sullivan, O. S., Horswill, P., Phoenix, G. K., Lee, J. A., & Leake, J. R. (2011). Recovery of soil nitrogen pools in species-rich grasslands after 12 years of simulated pollutant

1028 nitrogen deposition: A 6-year experimental analysis. *Global Change Biology*, *17*(8),
1029 2615–2628. https://doi.org/10.1111/j.1365-2486.2011.02403.x
1030 Ouyang, Y., Evans, S. E., Friesen, M. L., & Tiemann, L. K. (2018). Effect of nitrogen
1031 fertilization on the abundance of nitrogen cycling genes in agricultural soils: A meta-
1032 analysis of field studies. *Soil Biology and Biochemistry*, *127*(August), 71–78.
1033 https://doi.org/10.1016/j.soilbio.2018.08.024
1034 Penuelas, J., Fernández-Martínez, M., Vallicrosa, H., Maspons, J., Zuccarini, P., Carnicer, J.,
1035 Sanders, T. G. M., Krüger, I., Obersteiner, M., Janssens, I. A., Ciais, P., & Sardans, J.
1036 (2020). Increasing atmospheric CO2 concentrations correlate with declining nutritional
1037 status of European forests. *Communications Biology*, *3*(1), 125.
1038 https://doi.org/10.1038/s42003-020-0839-y
1039 Perakis, S. S., Sinkhorn, E. R., & Compton, J. E. (2011). δ15N constraints on long-term nitrogen
1040 balances in temperate forests. *Oecologia*, *167*(3), 793–807.
1041 https://doi.org/10.1007/s00442-011-2016-y
1042 Phillips, R. P., Brzostek, E., & Midgley, M. G. (2013). The mycorrhizal-associated nutrient
1043 economy: A new framework for predicting carbon–nutrient couplings in temperate
1044 forests. *New Phytologist*, *199*(1), 41–51. https://doi.org/10.1111/nph.12221
1045 Redfield, A. C. (1958). The biological control of chemical factors in the environment. *American*
1046 *Scientist*, *46*(3). https://www.jstor.org/stable/27827150
1047 Redling, K., Elliott, E., Bain, D., & Sherwell, J. (2013). Highway contributions to reactive
1048 nitrogen deposition: Tracing the fate of vehicular NOx using stable isotopes and plant
1049 biomonitors. *Biogeochemistry*, *116*(1–3), 261–274. https://doi.org/10.1007/s10533-013-
1050 9857-x

Riggs, C. E., & Hobbie, S. E. (2016). Mechanisms driving the soil organic matter decomposition response to nitrogen enrichment in grassland soils. *Soil Biology and Biochemistry*, *99*, 54–65. https://doi.org/10.1016/j.soilbio.2016.04.023

Robertson, G. P., Coleman, D. C., Bledsoe, C. S., & Sollins, P. (1999). *Standard Soil Methods for Long-Term Ecological Research*. Oxford University Press.

Robertson, G. P., & Groffman, P. M. (2015). Nitrogen Transformations. In *Soil Microbiology, Ecology and Biochemistry* (pp. 421–446). Elsevier. https://doi.org/10.1016/B978-0-12-415955-6.00014-1

Rocci, K. S., Cotrufo, M. F., & Baron, J. S. (2023). Proximity to Roads Does Not Modify Inorganic Nitrogen Deposition in a Topographically Complex, High Traffic, Subalpine Forest. *Water, Air, & Soil Pollution*, *234*(12), 761. https://doi.org/10.1007/s11270-023-06762-2

Rutz, C., Loretto, M.-C., Bates, A. E., Davidson, S. C., Duarte, C. M., Jetz, W., Johnson, M., Kato, A., Kays, R., Mueller, T., Primack, R. B., Ropert-Coudert, Y., Tucker, M. A., Wikelski, M., & Cagnacci, F. (2020). COVID-19 lockdown allows researchers to quantify the effects of human activity on wildlife. *Nature Ecology & Evolution*, *4*(9), 1156–1159. https://doi.org/10.1038/s41559-020-1237-z

Sabo, R. D., Elmore, A. J., Nelson, D. M., Clark, C. M., Fisher, T., & Eshleman, K. N. (2020). Positive correlation between wood δ^{15}N and stream nitrate concentrations in two temperate deciduous forests. *Environmental Research Communications*, *2*(2), 025003. https://doi.org/10.1088/2515-7620/ab77f8

Saiya-Cork, K. R., Sinsabaugh, R. L., & Zak, D. R. (2002). The effects of long term nitrogen deposition on extracellular enzyme activity in an Acer saccharum forest soil. *Soil Biology and Biochemistry*, *34*(9), 1309–1315. https://doi.org/10.1016/S0038-0717(02)00074-3

Schimel, J. P., & Bennett, J. (2004). Nitrogen mineralization: Challenges of a changing paradigm. *Ecology*, *85*(3), 591–602. https://doi.org/10.1890/03-8002

Schimel, J. P., & Weintraub, M. N. (2003). The implications of exoenzyme activity on microbial carbon and nitrogen limitation in soil: A theoretical model. *Soil Biology and Biochemistry*, *35*(4), 549–563. https://doi.org/10.1016/S0038-0717(03)00015-4

Schlesinger, W. H. (2009). On the fate of anthropogenic nitrogen. *Proceedings of the National Academy of Sciences*, *106*(1), 203–208. https://doi.org/10.1073/pnas.0810193105

Schrimpf, M. B., Des Brisay, P. G., Johnston, A., Smith, A. C., Sánchez-Jasso, J., Robinson, B. G., Warrington, M. H., Mahony, N. A., Horn, A. G., Strimas-Mackey, M., Fahrig, L., & Koper, N. (2021). Reduced human activity during COVID-19 alters avian land use across North America. *Science Advances*, *7*(39), eabf5073. https://doi.org/10.1126/sciadv.abf5073

Schwede, D. B., & Lear, G. G. (2014). A novel hybrid approach for estimating total deposition in the United States. *Atmospheric Environment*, *92*, 207–220. https://doi.org/10.1016/j.atmosenv.2014.04.008

Shipley, B. (2013). The AIC model selection method applied to path analytic models compared using a d-separation test. *Ecology*, *94*(3), 560–564. https://doi.org/10.1890/12-0976.1

Sinsabaugh, R. L., & Follstad Shah, J. J. (2012). Ecoenzymatic Stoichiometry and Ecological Theory. *Annual Review of Ecology, Evolution, and Systematics*, *43*(1), 313–343. https://doi.org/10.1146/annurev-ecolsys-071112-124414

Sinsabaugh, R. L., Hill, B. H., & Follstad Shah, J. J. (2009). Ecoenzymatic stoichiometry of microbial organic nutrient acquisition in soil and sediment. *Nature*, *462*(7274), 795–798. https://doi.org/10.1038/nature08632

Sinsabaugh, R. L., Lauber, C. L., Weintraub, M. N., Ahmed, B., Allison, S. D., Crenshaw, C., Contosta, A. R., Cusack, D., Frey, S., Gallo, M. E., Gartner, T. B., Hobbie, S. E., Holland, K., Keeler, B. L., Powers, J. S., Stursova, M., Takacs-Vesbach, C., Waldrop, M. P., Wallenstein, M. D., … Zeglin, L. H. (2008). Stoichiometry of soil enzyme activity at global scale. *Ecology Letters*, *11*(11), 1252–1264. https://doi.org/10.1111/j.1461-0248.2008.01245.x

Sinsabaugh, R. S. (1994). Enzymic analysis of microbial pattern and process. *Biology and Fertility of Soils*, *17*(1), 69–74. https://doi.org/10.1007/BF00418675

Soong, J. L., Fuchslueger, L., Marañon-Jimenez, S., Torn, M. S., Janssens, I. A., Penuelas, J., & Richter, A. (2020). Microbial carbon limitation: The need for integrating microorganisms into our understanding of ecosystem carbon cycling. *Global Change Biology*, *26*(4), 1953–1961. https://doi.org/10.1111/gcb.14962

Soto, E. H., Botero, C. M., Milanés, C. B., Rodríguez-Santiago, A., Palacios-Moreno, M., Díaz-Ferguson, E., Velázquez, Y. R., Abbehusen, A., Guerra-Castro, E., Simoes, N., Muciño-Reyes, M., & Filho, J. R. S. (2021). How does the beach ecosystem change without tourists during COVID-19 lockdown? *Biological Conservation*, *255*, 108972. https://doi.org/10.1016/j.biocon.2021.108972

Stevens, C. J. (2016). How long do ecosystems take to recover from atmospheric nitrogen deposition? *Biological Conservation*, *200*, 160–167. https://doi.org/10.1016/j.biocon.2016.06.005

Stienstra, A. W., Klein Gunnewiek, P., & Laanbroek, H. J. (1994). Repression of nitrification in soils under a climax grassland vegetation. *FEMS Microbiology Ecology*, *14*(1), 45–52. https://doi.org/10.1111/j.1574-6941.1994.tb00089.x

Tatsumi, C., Taniguchi, T., Du, S., Yamanaka, N., & Tateno, R. (2020). Soil nitrogen cycling is determined by the competition between mycorrhiza and ammonia-oxidizing prokaryotes. *Ecology*, *101*(3), e02963. https://doi.org/10.1002/ecy.2963

Treseder, K. K. (2008). Nitrogen additions and microbial biomass: A meta-analysis of ecosystem studies. *Ecology Letters*, *11*(10), 1111–1120. https://doi.org/10.1111/j.1461-0248.2008.01230.x

Vega Anguiano, N., Freeman, K. M., Figge, J. D., Hawkins, J. H., & Zeglin, L. H. (2024). Bison and cattle grazing increase soil nitrogen cycling in a tallgrass prairie ecosystem. *Biogeochemistry*. https://doi.org/10.1007/s10533-024-01144-0

Venables, W. N., & Ripley, B. D. (2002). *Modern applied statistics with S* (4th ed). Springer.

Verhagen, F. J. M., Laanbroek, H. J., & Woldendrop, J. W. (1995). Competition for ammonium between plant roots and nitrifying and heterotrophic bacteria and the effects of protozoan grazing. *Plant and Soil*, *170*, 241–250. https://doi.org/10.1007/BF00010477

Vitousek, P. M., Aber, J. D., Howarth, R. W., Likens, G. E., Matson, P. A., Schindler, D. W., Schlesinger, W. H., & Tilman, D. G. (1997). Human alteration of the global nitrogen cycle: Sources and consequences. *Ecological Applications*, *7*(3), 737–750.

Von Holle, B., Neill, C., Largay, E. F., Budreski, K. A., Ozimec, B., Clark, S. A., & Lee, K. (2013). Ecosystem legacy of the introduced N2-fixing tree Robinia pseudoacacia in a coastal forest. *Oecologia*, *172*(3), 915–924. https://doi.org/10.1007/s00442-012-2543-1

Wickham, H., Averick, M., Bryan, J., Chang, W., McGowan, L., François, R., Grolemund, G., Hayes, A., Henry, L., Hester, J., Kuhn, M., Pedersen, T., Miller, E., Bache, S., Müller, K., Ooms, J., Robinson, D., Seidel, D., Spinu, V., … Yutani, H. (2019). Welcome to the Tidyverse. *Journal of Open Source Software*, *4*(43), 1686. https://doi.org/10.21105/joss.01686

Yang, M., Chen, L., Msigwa, G., Tang, K. H. D., & Yap, P.-S. (2022). Implications of COVID-19 on global environmental pollution and carbon emissions with strategies for sustainability in the COVID-19 era. *Science of The Total Environment*, *809*, 151657. https://doi.org/10.1016/j.scitotenv.2021.151657

Yuan, X., Niu, D., Gherardi, L. A., Liu, Y., Wang, Y., Elser, J. J., & Fu, H. (2019). Linkages of stoichiometric imbalances to soil microbial respiration with increasing nitrogen addition: Evidence from a long-term grassland experiment. *Soil Biology and Biochemistry*, *138*, 107580. https://doi.org/10.1016/j.soilbio.2019.107580

Zeglin, L. H., Stursova, M., Sinsabaugh, R. L., & Collins, S. L. (2007). Microbial Responses to Nitrogen Addition in Three Contrasting Grassland Ecosystems. *Oecologia*, *154*(2), 349–359. https://doi.org/10.1007/s00442-007-0836-6

Table S1 | List of regions and sites used for the study.

Region	Site	# of plots	Ecosystem	Latitude, Longitude[†]	Mean annual N deposition (kg N ha^{-1})	N deposition class	Mean annual precipitation (mm)	Mean annual temperature (ºC)	Climate	Dominant vegetation[°]	Yard management
CA	Annual Grassland	1	Grassland	33º44' N, 117º42' W	6.93	Low	332	19.3	Xeric	*Avena fatua*, *Bromus diandrus*	-
	Coastal Sage Scrub	1	Scrub	33º44' N, 117º42' W	6.93	Low	332	19.3	Xeric	*Malosma laurina*	-
	Yard	2	Yard	33º N, 117º W	5.60	Low	284	18.3	Xeric	Native forbs, grasses, and shrubs	Small amount of fertilization once a year; Limited drip irrigation during dry season
E. MA	Deciduous Forest	2	Deciduous Forest	42º19' N, 71º10' W	8.81	High	1254	10.7	Mesic	*Acer rubrum*, *Betula lenta*, *Quercus rubra*	-
	Mixed Deciduous Forest	2	Deciduous Forest	42º19' N, 71º10' W	6.38	Low	1254	10.7	Mesic	*Acer rubrum*, *Pinus strobus*, *Quercus rubra*	-
FL	Subtropical Pine Forest	1	Coniferous Forest	28º4' N, 82º23' W	7.53	Intermediate	1257	23.6	Mesic	*Pinus elliottii*, *Pinus palustris*, *Quercus* spp.	-
	Subtropical Oak-Palmetto Forest	1	Oak-Palmetto Forest	28º4' N, 82º23' W	7.53	Intermediate	1257	23.6	Mesic	*Serenoa repens*, *Quercus* spp.	-
	Yard	1	Yard	28º N, 82º W	7.82	Intermediate	1257	23.6	Mesic	Turfgrass and forbs	No fertilization, irrigation, or pesticide use; Occasional mowing
ID	Palouse Prairie	1	Grassland	46º40' N, 116º58' W	4.58	Low	706	8.0	Xeric	*Balsamorhiza sagittate*, *Festuca idahoensis*, *Pseudoroegneria spicata*	-
	Western Dry	1	Coniferous Forest	46º40' N, 116º58' W	4.58	Low	706	8.0	Xeric	*Pinus ponderosa*	-

	Coniferous Forest										
	Yard	1	Yard	47º N, 117º W	4.63	Low	706	8.0	Xeric	Turfgrass	No current fertilization, pesticide use, or irrigation, infrequent mowing
MN	Mixed Deciduous Forest	3	Deciduous Forest	45º25’ N, 93º11’ W	9.86	High	753	6.7	Mesic	*Acer rubrum*, *Quercus ellipsoidalis*	-
	Old Field Grassland	3	Grassland	45º25’ N, 93º11’ W	9.86	High	753	6.7	Mesic	*Schizachyrium scoparium*	-
	Yard	1	Yard	45º N, 93º W	10.45	High	831	7.1	Mesic	*Poa pratensis*	No fertilization, occasional irrigation
MT	Semiarid Grassland	3	Grassland	47º4’ N, 113º14’ W	3.18	Low	549	5.4	Xeric	Native and introduced bunchgrass spp.	-
	Western Dry Coniferous Forest	3	Coniferous Forest	47º4’ N, 113º14’ W	3.18	Low	549	5.4	Xeric	*Pinus ponderosa*, *Pseudotsuga menziesii*	-
N. CT	Mixed Forest	3	Deciduous Forest	41º59’ N, 72º7’ W	8.02	Intermediate	1275	8.4	Mesic	*Acer rubrum*, *Betula lenta*, *Pinus strobus*, *Tsuga canadensis*, *Quercus rubra*	-
	Yard	1	Yard	42º N, 72º W	8.07	Intermediate	1275	8.4	Mesic	Turfgrass, *Trifolium* spp.	No fertilization or irrigation
NH	Mixed Deciduous Forest	1	Deciduous Forest	43º10’ N, 71º13’ W	5.65	Low	1176	8.6	Mesic	*Acer rubrum*, *Fagus grandifolia*, *Pinus* spp., *Quercus* spp.	-
	Yard	1	Yard	43º N, 71º W	5.65	Low	1176	8.6	Mesic	Turfgrass	No fertilization or irrigation; Occasional mowing
NY	Alley Pond	1	Deciduous Forest	40º44’ N, 73º44’ W	11.67	High	1100	12.4	Mesic	n/a	-
	Bethpage	1	Deciduous Forest	40º45’ N, 73º28’ W	8.28	Intermediate	972	11.9	Mesic	n/a	-
	Edgewood	1	Scrub	40º46’ N, 73º18’ W	7.68	Intermediate	972	11.9	Mesic	*Pinus rigida*, *Quercus* spp.	-

	Hempstead	1	Deciduous Forest	40º40’ N, 73º38’ W	8.56	High	1100	12.4	Mesic	n/a	-
	Yard	1	Yard	40º N, 73º W	8.45	Intermediate	972	11.9	Mesic	n/a	No fertilization; Occasional mowing
OH	Blendon	1	Deciduous Forest	40º4’ N, 82º52’ W	9.90	High	1073	12.2	Mesic	*Fagus grandifolia*, *Quercus alba*	-
	Wooster	1	Deciduous Forest	39º59’ N, 82º59’ W	9.42	High	1134	11.6	Mesic	*Carya ovata*, *Quercus alba*	-
	Yard	1	Yard	41º N, 83º W	9.33	High	889	11.2	Mesic	Turfgrass and forbs	No fertilization, irrigation, or pesticide use
OR	Western Wet Coniferous Forest	2	Coniferous Forest	44º37’ N, 123º21’ W	3.78	Low	1093	11.6	Mesic	*Abies grandis*, *Acer macrophyllum*, *Pseudotsuga menziesii*	-
	Yard	1	Yard	44º N, 123º W	3.78	Low	1093	11.6	Mesic	Turfgrass and forbs	No current fertilization, irrigation, or pesticide use; Occasional mowing
PA	Suburban Forest	3	Deciduous Forest	40º32’ N, 79º54’ W	10.10	High	1131	10.5	Mesic	*Acer* spp., *Prunus serotina*, *Quercus* spp	-
	Urban Forest	3	Deciduous Forest	40º25’ N, 79º56’ W	7.77	Intermediate	1031	11.3	Mesic	*Acer* spp., *Liriodendron tulipifera*, *Quercus* spp.	-
	Yard	1	Yard	40º N, 80º W	7.77	Intermediate	1031	10.5	Mesic	Turfgrass, *Trifolium repens*	No fertilization or irrigation; Infrequent mowing
S. CT	Maple Beech Birch	3	Deciduous Forest	41º20’ N, 72º57’ W	8.96	High	1280	10.9	Mesic	*Acer rubrum*, *Betula lenta*, *Fagus grandifolia*	
	Oak-Hickory	3	Deciduous Forest	41º20’ N, 72º58’ W	8.96	High	1280	10.9	Mesic	*Carya glabra*, *Juniperus virginiana*, *Quercus* spp.	
	Yard	1	Yard	41º N, 72º W	8.96	High	1280	10.9	Mesic	Turfgrass	No fertilization or irrigation; Regular

											mowing and maintenance
W. MA	Hardwood	2	Deciduous Forest	42°22'N 72°25'W	7.66	Intermediate	1183	9.0	Mesic	*Acer* spp., *Betula* spp., *Fagus grandifolia*, *Quercus* spp.	-
	Pine	2	Coniferous Forest	42°22'N 72°25'W	7.66	Intermediate	1183	9.0	Mesic	*Picea* spp., *Pinus* spp., *Tsuga canadensis*	-
	Yard	1	Yard	42° N 72° W	7.66	Intermediate	1183	9.0	Mesic	Turfgrass, *Trifolium* spp.	No current fertilization or irrigation

[†]Longitude and latitude coordinates for Yard sites are inexact for privacy.

°Species listed in alphabetical order.

Table S2 | Rationale for model paths for hypothesized structural equation model (SEM) (Fig. S2) prior to fitting data to model. We included the hypothesized path of enzymatic C:N explained by soil pH to justify its inclusion in the final SEM.

Response variable	Explanatory variable	Justification
Active microbial biomass (SIR)	Soil C	Bradford et al., 2008
Enzymatic C:N	Soil C	Sinsabaugh et al., 2014
	Soil N	Sinsabaugh et al., 2014
	Soil pH	Sinsabaugh et al., 2008
$f_{\text{nitrified}}$	Active microbial biomass (SIR)	Li et al., 2021
	Enzymatic C:N	Vega Anguiano et al., 2024
	Soil pH	Petersen et al., 2012
	Soil moisture (GWC)	Gill et al., 2023
	Soil C	Keiser et al., 2016
	Soil N	Petersen et al., 2012

Bradford, M. A., Fierer, N., & Reynolds, J. F. (2008). Soil carbon stocks in experimental mesocosms are dependent on the rate of labile carbon, nitrogen and phosphorus inputs to soils. *Functional Ecology*, *22*(6), 964–974. https://doi.org/10.1111/j.1365-2435.2008.01404.x

Gill, A. L., Grinder, R. M., See, C. R., Chapin, F. S., DeLancey, L. C., Fisk, M. C., Groffman, P. M., Harms, T., Hobbie, S. E., Knoepp, J. D., Knops, J. M. H., Mack, M., Reich, P. B., & Keiser, A. D. (2023). Soil carbon availability decouples net nitrogen mineralization and net nitrification across United States Long Term Ecological Research sites. *Biogeochemistry*, *162*(1), 13–24. https://doi.org/10.1007/s10533-022-01011-w

Keiser, A. D., Knoepp, J. D., & Bradford, M. A. (2016). Disturbance Decouples Biogeochemical Cycles Across Forests of the Southeastern US. *Ecosystems*, *19*(1), 50–61. https://doi.org/10.1007/s10021-015-9917-2

Li, Z., Zeng, Z., Song, Z., Wang, F., Tian, D., Mi, W., Huang, X., Wang, J., Song, L., Yang, Z., Wang, J., Feng, H., Jiang, L., Chen, Y., Luo, Y., & Niu, S. (2021). Vital roles of soil microbes in driving terrestrial nitrogen immobilization. *Global Change Biology*, *27*(9), 1848–1858. https://doi.org/10.1111/gcb.15552

Petersen, D. G., Blazewicz, S. J., Firestone, M., Herman, D. J., Turetsky, M., & Waldrop, M. (2012). Abundance of microbial genes associated with nitrogen cycling as indices of biogeochemical process rates across a vegetation gradient in Alaska. *Environmental Microbiology*, *14*(4), 993–1008. https://doi.org/10.1111/j.1462-2920.2011.02679.x

Sinsabaugh, R. L., Belnap, J., Findlay, S. G., Shah, J. J. F., Hill, B. H., Kuehn, K. A., Kuske, C. R., Litvak, M. E., Martinez, N. G., Moorhead, D. L., & Warnock, D. D. (2014). Extracellular enzyme kinetics scale with resource availability. *Biogeochemistry*, *121*(2), 287–304. https://doi.org/10.1007/s10533-014-0030-y

Sinsabaugh, R. L., Lauber, C. L., Weintraub, M. N., Ahmed, B., Allison, S. D., Crenshaw, C., Contosta, A. R., Cusack, D., Frey, S., Gallo, M. E., Gartner, T. B., Hobbie, S. E., Holland, K., Keeler, B. L., Powers, J. S., Stursova, M., Takacs-Vesbach, C., Waldrop, M. P., Wallenstein, M. D., … Zeglin, L. H. (2008). Stoichiometry of soil enzyme activity at global scale. *Ecology Letters*, *11*(11), 1252–1264. https://doi.org/10.1111/j.1461-0248.2008.01245.x

Vega Anguiano, N., Freeman, K. M., Figge, J. D., Hawkins, J. H., & Zeglin, L. H. (2024). Bison and cattle grazing increase soil nitrogen cycling in a tallgrass prairie ecosystem. *Biogeochemistry*. https://doi.org/10.1007/s10533-024-01144-0

Table S3 | Model outputs of net N transformations with different soil microbial functional attributes. Bolded lines separate the different models. Values in cells are the *F*-, *P*-values.

	Enzymatic C:N ratio	**N deposition classification**	**Interaction**
Net nitrification	**10.52, 0.002**	1.61, 0.207	0.49, 0.614
Net N mineralization°	**5.04, 0.028**	**3.85, 0.026**	0.33, 0.721
$f_{\text{nitrified}}$	**24.82, < 0.001**	1.20, 0.308	0.02, 0.981
	NAG activity	**N deposition classification**	**Interaction**
Net nitrification°	**4.10, 0.047**	0.40, 0.672	**3.21, 0.046**
Net N mineralization	0.36, 0.551	**4.32, 0.017**	**4.12, 0.020**
$f_{\text{nitrified}}$	**5.89, 0.018**	1.15, 0.321	**5.06, 0.009**
	Active microbial biomass (SIR)	**N deposition classification**	**Interaction**
Net nitrification	1.35, 0.249	0.81, 0.447	2.21, 0.118
Net N mineralization	0.17, 0.685	**4.43, 0.015**	**5.09, 0.009**
$f_{\text{nitrified}}$	**4.71, 0.033**	0.77, 0.469	2.30, 0.107

° Yeo-Johnson-transformation

Fixed effects with *P*-values less 0.05 are bolded.

Table S4 | Model outputs of net N transformations to test for differences between years 2020 and 2021. Values in cells are the *F*-, *P*-values.

	Site (S)	Time (T)	Year (Y)	S × T	S × Y	T × Y	S × T × Y
Net N mineralization	2.04, 0.127	0.84, 0.475	3.23, 0.076	1.30, 0.207	**4.65, < 0.001**	0.78, 0.509	1.11, 0.356
Net nitrification°	**60.22, < 0.001**	**7.11, < 0.001**	**16.67, < 0.001**	**2.03, 0.016**	**2.99, 0.011**	2.40, 0.073	**1.85, 0.040**

° Yeo-Johnson-transformation

Fixed effects with *P*-values less 0.05 are bolded.

Figure S1 | The CASTNET stations surveyed for dry N deposition rates from 2013-2021. Shapes of the points correspond to background N deposition classification at low (circles), intermediate (squares), and high (triangles). Names of the CASTNET station are the following: JOT403, Joshua Tree NP; GLR468, Glacier NP; IRL141, Indian River Lagoon; LRL117, Laurel Hill; PRK134, Perkinstown; and QAK172, Quaker City.

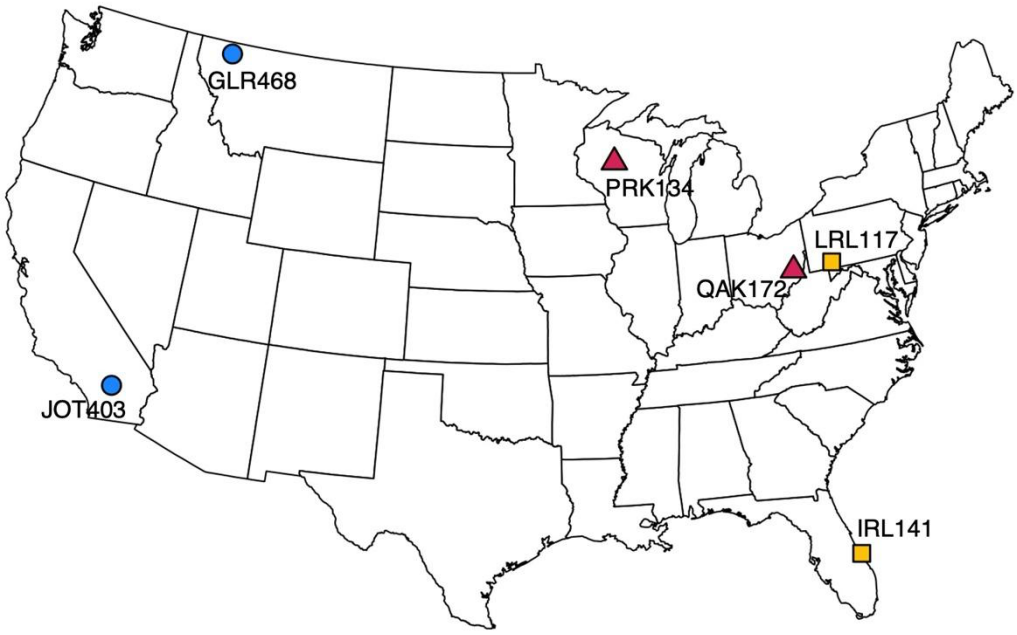

Figure S2 | Hypothesized structural equation model designed *a priori* before fitting data. See Table S2 for justifications of paths.

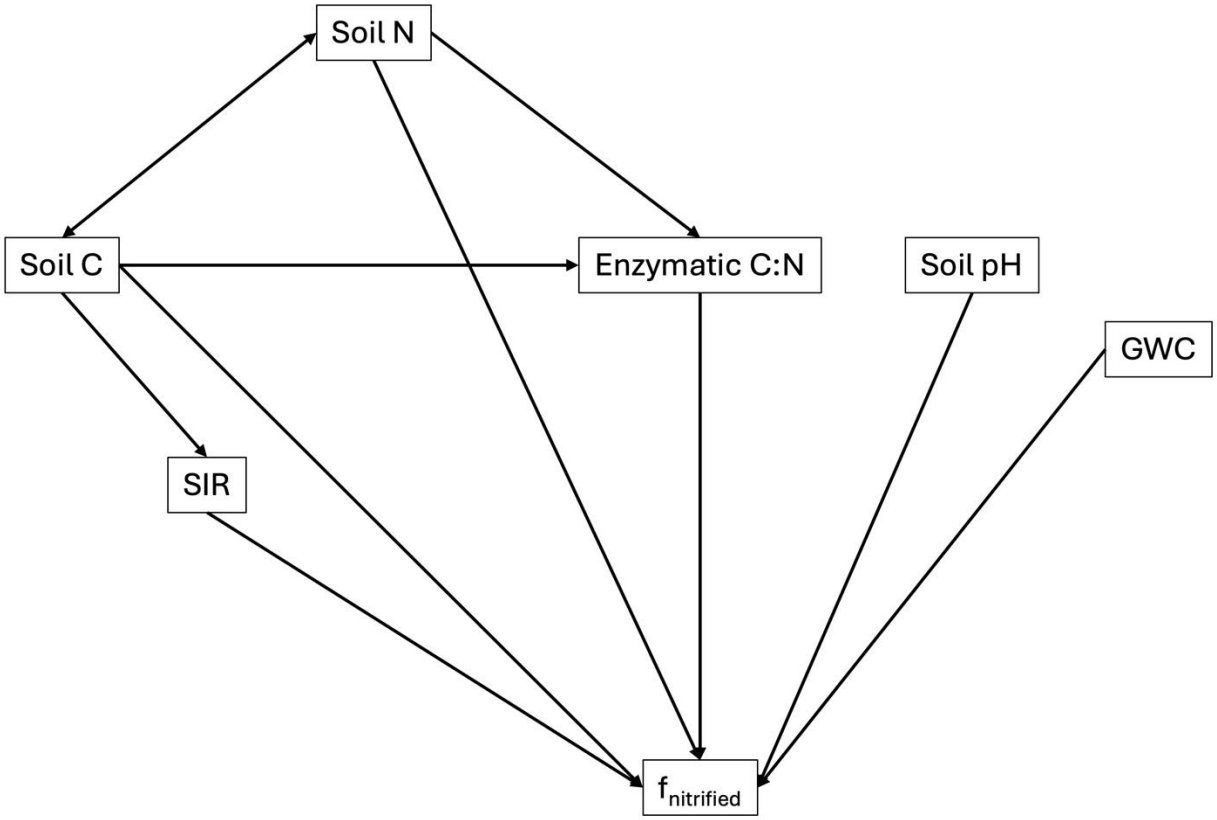

Figure S3 | Cumulative dry N deposition for six CASTNET stations across the United States categorized based on N deposition class ranks. Line colors correspond to year. Shaded areas for the 2013-2017 average are the 95% confidence interval. Locations of CASTNET stations with the U.S. are found in Fig. S1. Names of the CASTNET station are the following: JOT403, Joshua Tree NP; GLR468, Glacier NP; IRL141, Indian River Lagoon; LRL117, Laurel Hill; PRK134, Perkinstown; and QAK172, Quaker City.

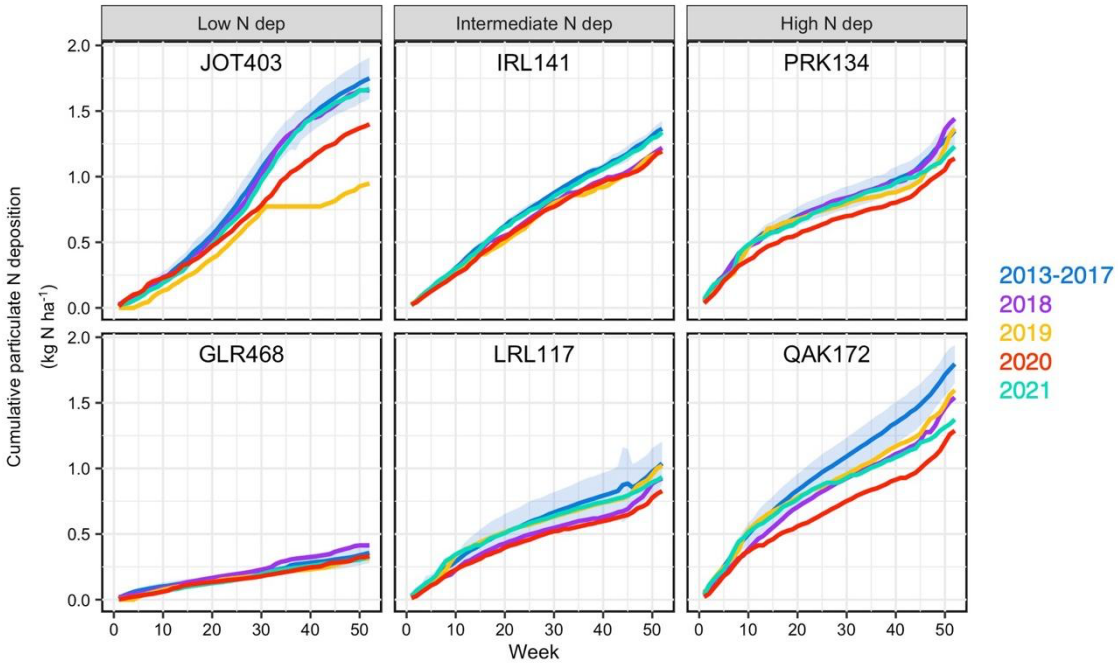

Figure S4 | Interactions between net N mineralization rates and (a) soil C:N ratio, (b) soil pH, and (c) soil moisture for the best fitting soil characteristics model to explain net nitrification rates (model in Table 2). Each line corresponds to the first quartile, mean, and third quartile of the soil chemistry variable. Values of the soil chemistry variables are listed adjacent to lines in the legends.

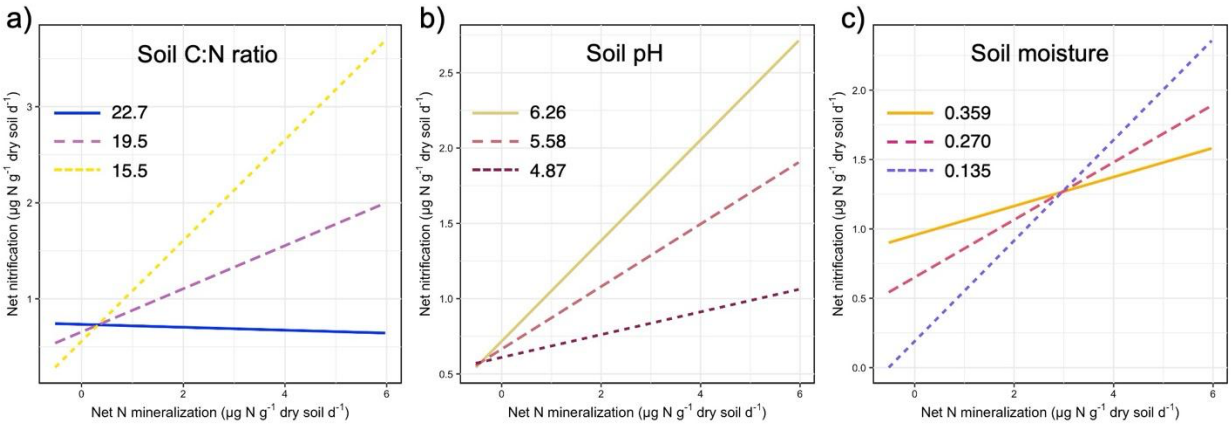

Figure S5 | Responses of (a) soil pH, (b) soil %C, (c) soil %N, and (d) soil C:N to background N deposition, split by different ecosystems (n = 69). Each point is the soil chemistry parameter for a site at each collection time. Letters within an ecosystem type denote post-hoc differences at $P <$ 0.05 among background N deposition classes.

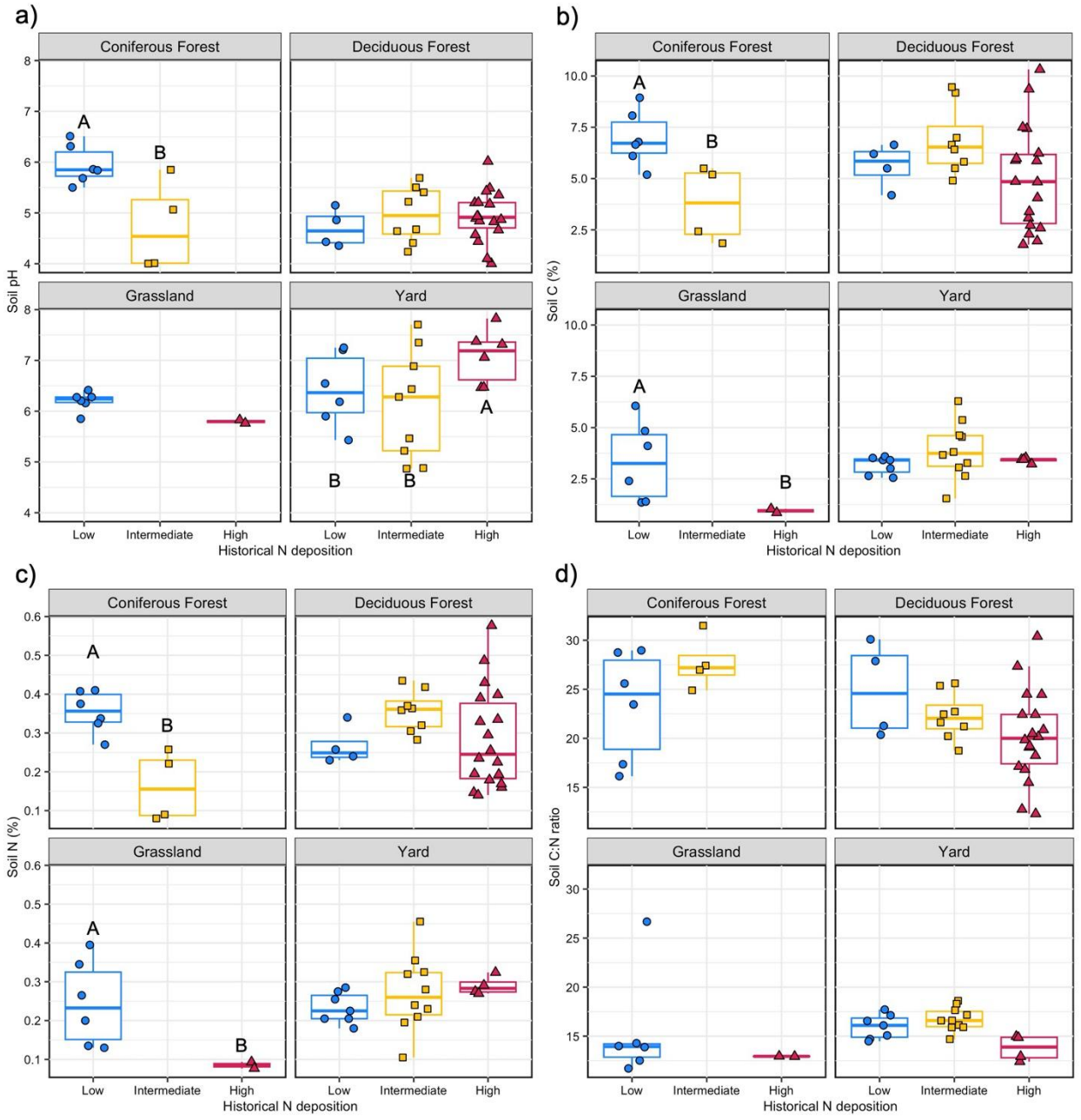

Figure S6 | The relationship of (a) net nitrification, (b) net N mineralization, and (c) $f_{\text{nitrified}}$ with log NAG activity. Each point is the net N transformation rate or $f_{\text{nitrified}}$ for each site at a collection time colored (n = 78). Line colors correspond to background N deposition classification, showing the significant (solid) or insignificant (dotted) correlations between the N-cycling metrics and NAG activity.